Martin G. Rausch, BSc.

Enhancing the Thermal Conductivity of Epoxide Resins with Boron Nitride Nanofillers

MASTER'S THESIS

to achieve the university degree of

Diplom-Ingenieur

Master's degree programme: Technical Chemistry

submitted to

Graz University of Technology

Supervisor

Priv.-Doz. Dr.rer.nat. Dipl.-Chem.Univ. Wiesbrock Frank

Institute for Chemistry and Technology of Materials

Univ.-Prof. Dipl.-Ing. Dr.techn. Stelzer Franz

Graz, August 2016

AFFIDAVIT

I declare that I have authored this thesis independently, that I have not used other than the declared sources/resources, and that I have explicitly indicated all material which has been quoted either literally or by content from the sources used. The text document uploaded to TUGRAZonline is identical to the present master's thesis.

GRAZ, 30.08.2016
_____
Date

_____
Signature

…für meine Eltern!

Danke für eure Unterstützung über die vielen Jahre.
Ihr habt mir diese Arbeit erst möglich gemacht.

Table of Content

List of figures

List of abbreviations

Acknowledgement

First and foremost, I have to thank my parents for their support and guidance that they gave throughout the years in a selfless manner like just parents can do. Without their great effort and time that they spent for my education from the first days of my life onwards I could not be where I am today. Actually, you two are the best parents I could possibly imagine.

I would like to thank Priv.-Doz. Frank Wiesbrock for the provision of the interesting topic, the scientific freedom and his expertise and time he generously spent on the mentoring and supervision of this work.

I have to acknowledge Zucong Zhang for the SEM/EDX and permittivity measurements and his knowledge he generously gave, Petra Kaschnitz for her time and expertise she spent into the boron NMR measurements, Andrea Wanner and Philipp Marx for the heat conductivity measurements, Angela Chemelli for her time and goodwill throughout the DLS measurements, Klaus Reichmann for his time and the pyrolysis of polyborazine, Roland Fischer for his efforts during crystal structure analyses, and Thomas Grießer for the XPS analysis.

I want to thank my colleagues in the office, the group and the whole institute for their support and awesome time they gave me during this work. It has been a pleasure!

Last but not the least, I have to thank Lisa for her support she gave me in times when the work seemed never ending and impossible. I truly appreciate your kindness, love and patience you give and hope to be able to give back at least a bit of it.

Abstract

The aim of this work was to improve the heat conductivity of an epoxide-anhydride resin system by the addition of suitable filler material. Intensive research about state-of-the-art techniques for increasing the heat conductivity of polymer films led to the choice of boron nitride nanoparticles.

In order to gain an overview about possible benefits and difficulties of a full synthesis of boron nitride, a polymer-derived ceramic pathway was chosen to mimic the whole process from inexpensive starting materials to BN as possible polymer additive. Starting from $(NH_4)_2SO_4$ and $NaBH_4$, the reaction in a suitable solvent led to the formation of borazine $B_3N_3H_6$, a six-membered heterocycle with alternating boron and nitrogen atoms. Due to its volatility, a polymerization before its subsequent pyrolysis was necessary. It was shown that the reaction conditions are crucial for the final success of the synthesis of borazine, polyborazines and boron nitride, revealing the high sensitivity of the chosen method. These facts render this strategy less recommendable for commercial use.

Commercially available boron nitride nanopowder was fully characterized using SEM/EDX, XPS, DLS and ATR/IR investigations, revealing an average particle size of around 140 nm. Samples with different weight loads of boron nitride in an Araldite CY225 / Aradur HY925 epoxide resin system were produced and characterized. The thermal conductivity could be increased by up to 40% for a 25 wt.-% filler loading compared to the pristine epoxide-anhydride resin. With special respect to the balance between processing properties and thermal performance, a weight load of 10 wt.-% BN seems suitable, still increasing the thermal conductivity by up to 20%.

In addition to their heat conductivity properties, a possible change in the electrical permittivity was investigated. All resins and composites (with filler loads of 0, 10, and 25 wt.-% BN) exhibited permittivity in the range of 3.6 to 4.0 over the whole range of frequencies investigated. With regard to water uptake under ambient conditions, no linear dependence could be drawn between the weight load and the moisture absorption capabilities. It was shown that the presence of boron nitride within an epoxide matrix increases the moisture uptake. The moisture absorption capabilities were highest at a weight load of 10 wt.-% BN and dropped for a higher loading of 25 wt.-%. Most likely, this appearance can be explained by agglomeration of the particles within the sample with a higher weight load, decreasing the surface of exposed boron nitride.

The occurrence of gas cavities in the composites can probably be explained with bad wetting properties of boron nitride and accompanying agglomeration. Due to this fact, the activation and modification of boron nitride with –OH groups seemed necessary. It could be shown that the material is inert against treatment with nitration acid at 80 °C for 72 h. The treatment of BN nanoparticles in piranha acid at 80 °C for 72 h seems to a promising strategy for activation, namely by surficial oxidization.

Kurzfassung

Das Ziel dieser Arbeit war die Erhöhung der thermischen Leitfähigkeit eines Epoxidharz-Anhydrid-Harzes durch den Einsatz geeigneter Füllermaterialien. Umfangreiche Recherchen über bekannte Methoden zur Erhöhung der thermischen Leitfähigkeit von Polymeren offenbarten das große Potential von Bornitrid in der Form von Nanopulver als Polymeradditiv.

Um einen Überblick über etwaige Vor- und Nachteile einer vollständigen Synthese von Bornitrid zu erhalten, wurde eine Synthesestrategie ausgewählt, die auf relativ günstigen Ausgangsverbindungen basiert. Ausgehend von Ammoniumsulfat $(NH_4)_2SO_4$ und Natriumborhydrid $NaBH_4$ wurde versucht, Borazin $B_3N_3H_6$ darzustellen. Dieser anorganische Sechsring besteht aus Bor und Stickstoff, welche in alternierender Reihenfolge auftreten. Aufgrund der hohen Flüchtigkeit der Verbindung ist eine direkte Pyrolyse zu Bornitrid nicht möglich; erst eine vorhergehende Polymerisierung zu Polyborazin macht diesen Schritt umsetzbar. Die Synthese von Borazin und Polyborazin gestaltete sich äußerst schwierig und es konnte gezeigt werden, dass es sich hierbei um eine äußerst komplexe Synthese handelt. Viele Parameter müssen korrekt eingestellt werden, um eine adäquate Ausbeute zu erreichen. Die vollständige selbständige Synthese von BN kann daher für die kommerzielle Nutzung nur bedingt empfohlen werden.

Kommerziell erhältliches Bornitrid-Nanopulver konnte vollständig mittels SEM/EDX, XPS, DLS und ATR/IR charakterisiert werden. Dabei konnte festgestellt werden, dass die durchschnittliche Partikelgröße bei etwa 140 nm lag. In der Folge wurden Probenkörper mit verschiedenen Massenanteilen BN hergestellt und untersucht. Als Matrixsystem wurde das Araldit CY225 / Aradur HY925 Epoxidharz gewählt.

Die thermische Leitfähigkeit des Harzes konnte mit einem Massenanteil von 25 wt.-% um etwa 40% im Vergleich zum unbehandelten Harz gesteigert werden. Ein Massenanteil von 10 wt.-% erwies sich als signifikant besser verarbeitbare Variante ohne auftretende Gaseinschlüsse, welche eine Steigerung der thermischen Leitfähigkeit von etwa 20% zur Folge hatte.

Neben der möglichen Auswirkung auf die thermische Leitfähigkeit wurden auch die Implikationen des Füllermaterials auf die elektrische Permittivität untersucht. Dabei zeigte sich, dass kein direkter linearer Zusammenhang zwischen Massenanteil des Füllers und der erreichbaren Permittivität hergestellt werden kann: Alle gemessenen Permittivitäten lagen in einem engen Bereich von 3.6 bis 4.0.

In einer Feuchteaufnahmestudie konnte kein proportionaler Zusammenhang zwischen Massenanteil des Füllers und der effektiven Feuchteaufnahme festgestellt werden. Generell konnte festgestellt werden, dass die Anwesenheit von Bornitrid in einer Epoxidharzmatrix zur Erhöhung der Feuchteaufnahme führt. Höchste Werte wurden dabei für 10 wt.-% BN erreicht; bei 25 wt.-% BN sank die Feuchteaufnahme. Dieser Umstand kann auf die Agglomeration der Partikel bei höheren Beladungen und der damit einhergehenden Verringerung der Oberfläche erklärt werden.

Aufgrund der auftretenden Gaseinschlüsse innerhalb der Proben wurde versucht, das Bornitrid-Nanopulver zu funktionalisieren. Hierbei zeigte sich, dass das Material gegenüber Nitriersäure auch unter harschen Reaktionsbedingungen inert ist. Die Behandlung mittels Piranha-Säure führte zu einer deutlichen Erhöhung der oberflächengebundenen OH-Gruppen, was mittel ATR-IR- und XPS-Messungen nachgewiesen werden konnte.

1. Introduction: Aims of this thesis

Dating back to 1965, Gordon E. Moore formulated a law that he nowadays describes as "self-fulfilling prophecy". He postulated that the number of transistors in an integrated circuit in average would double every two years – leaving the size of the IC unaltered.[1] Although his prognosis was thought to last just for one single decade after publication, the semiconductor industry took this prediction as their ultimate law for adequate growth and took its lead until 2012, when the pace slowly started to decrease to a "cadence […] closer to two and a half years than two" – a rate that should be more or less constant at least until 2017.[2]

The benefits of this ongoing miniaturization are apparent: more transistors lead to higher performance, more compact design, and greater mobility. Hence, it is not the semiconductor industry exclusively that takes advantage of this trend of downscaling. Electronic industries tend to build smaller components in nearly every field of applications – to mention transformers, generators, and charging devices as prominent examples.

Concomitant with the more compact design of devices and machinery, more heat is developed in a given volume, and increased thermal conductivity has to be delivered by the insulating materials involved for the assembly. As the thermal conductivity of epoxide resins for both, high voltage applications and small electronical device packaging, is likely to become '*one of the bottle-neck problems for the continuous development in electronic industries*'[3] in the close future, the goal of this work was to investigate strategies to increase the thermal conductivity of a given epoxide resin system. Their electronical properties, nonetheless, should not be altered to significant extent. Besides its technological feasibility, environmental considerations should be included in the work, hence excluding toxic and hazardous substances.

One prominent strategy for the enhancement of the thermal conductivity of insulating polymer resins is the preparation of the corresponding composites with nanoparticles. Among these nanoparticles, hexagonal boron nitride is considered to be one high-potential candidate due to its high thermal conductivity, despite the fact that the preparation of nanoparticles of this particularly hard material remains challenging.

Hence, this thesis aimed in detail at a systematic investigation of the synthesis of borazine from non-hazardous reactants, its polymerization and pyrolysis to yield hexagonal boron nitride, and the preparation of boron nitride / epoxy nanocomposites as well as their characterization. For the preparation of the nanocomposites, commercially available epoxy / anhydride resins and hexagonal boron nitride nanoparticles were employed, aiming at the provision of data to enable predictions of the applicability of such types of compounds.

Situated in the context of currently on-going international research activities, this thesis dedicatedly addressed the following topics:

- Polymer-based synthetic strategies for the preparation of boron nitride.
- Activation of (chemically quasi-inert) boron nitride.
- Permittivity of epoxy / BN nanocomposites (considering high loadings of BN).
- Water uptake of epoxy / BN nanocomposites (considering high loadings of BN).

Based on the findings, a critical evaluation of the current state-of-the-art should be drawn, aiming at the elucidation of potential future research directions in this field of research.

2. State-of-the-art knowledge

2.1 The need for thermally conducting but electrically insulating polymers

Besides its obvious benefits, technology faces major challenges when device sizes drop. One of the biggest issues inherent to structures in the micro- to nano-range is the generation of more heat in smaller spaces. Although organic polymers face multiple fields of application in electronic industry such as printed circuit boards, thermal interface materials and device bases/holders,[4,5] they are mostly considered as thermal insulators with thermal conductivities far less than 1 $Wm^{-1}K^{-1}$ (Table 1).[6] As long as the packaging size was sufficiently large, this yet was of no matter – but, at the current stage of development, this will become "*one of the bottle-neck problems for the continuous development in electronic industries.*"[3]

Table 1: Thermal conductivity of selected materials.

Medium	Thermal conductivity [W m^{-1} K^{-1}]	Medium	Thermal conductivity [W m^{-1} K^{-1}]	Medium	Thermal conductivity [W m^{-1} K^{-1}]
Air[7]	0.0262	Nat. rubber[8]	0.134	Graphene[9]	5000
Water[7]	0.609	Polystyrene[10]	0.17	h-BN[11]	600
Iron[7]	80.3	Epoxy resins[10]	0.20	Epoxy/30wt.-% h-BN[12]	1.178
Copper[7]	398	Polyethylene[10]	0.33-0.57	Epoxy/25vol% CNTs/25vol% GNPs[13]	7.30

One promising strategy to increase the thermal conductivity of polymeric (adhesive) films is the introduction of materials capable of high heat transfer in the form of particles, platelets and fibers in the nano- to micro-regime.[14] Those particles act as

fillers to form heat transfer pathways and can increase the heat conductivity significantly (Figure 1). If the particle size drops from the micro- to the nano-regime, the available surface of the particles increases; thus, interfacial effects become one of the most important properties.

Besides their shape and size, other parameters such as electronic conductivity, functional surface groups and the evolving structural properties concerning the possibilities to be introduced into a polymeric matrix are of high importance. Especially for the use as adhesives in generators and transformers, the additives used have to be electrically insulating.
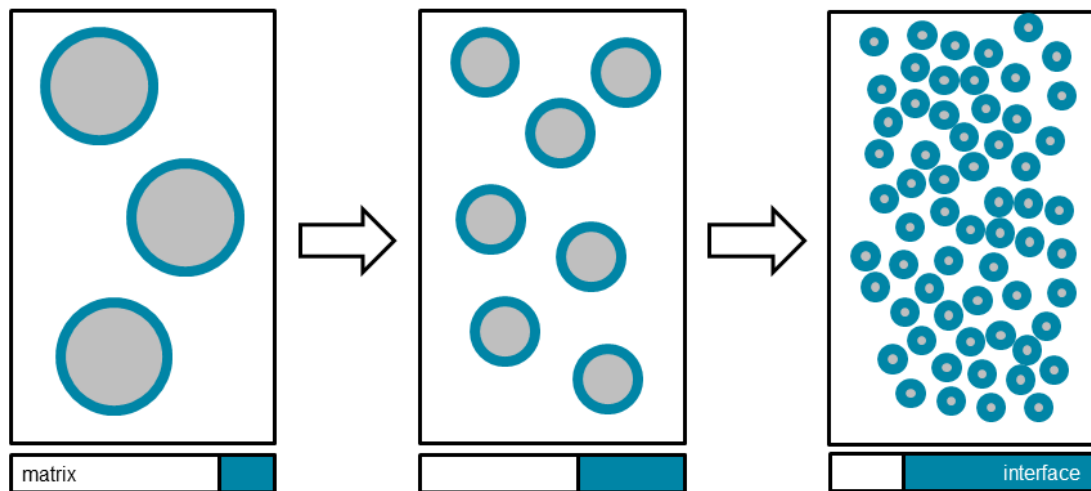
Figure 1: Correlation between particle size and interfacial region size.[15]

In addition to metal oxides such as Al_2O_3 and SiO_2, nitrides such as AlN and Si_3N_4, carbides such as SiC as well as graphene and its analogues (e.g., carbon nanotubes), non-oxide ceramics such as BN are the most promising candidates for the use as heat conductive additives in high-thermal-conductivity composites. For the use in electronic devices, the electric insulation ability of the organic polymers should not be altered, hence excluding the use of the electronic conductive fillers

such as graphene, carbon nanotubes (CNTs), SiC, Si_3N_4 and AlN, rendering BN (besides Al_2O_3 and SiO_2) one of the most promising candidates.[16]

In addition to the chemical composition, the appearance of the nanoparticles is of high importance (Figure 2). It may be distinguished between one- to three-dimensional structures, leading to different properties of the composite. For the use in thermally conductive composites, the choice of 2D-sheets seems adequate: Usage of a doctor blade for casting polymer films on surfaces induces shear forces that provide high degrees of orientation of the sheets within the matrix. This fact is of importance for an effective heat conduction.

| 1D | 2D | 3D |
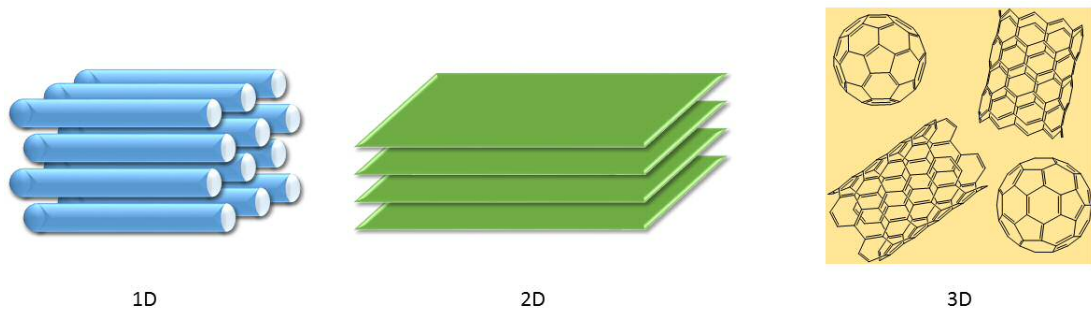
Figure 2: Possible structures of nanoparticles: 1-dimensional fibres, 2-dimensional sheets and 3-dimensional structures.

2.2 'White graphite' as nanofiller – a short introduction to boron nitride

Boron nitride as a III-V compound consisting of nitrogen and boron is isostructural and isoelectronic to carbon (Figure 3) and, like in the case of its carbon counterpart, shows three different crystalline forms: (i) hexagonal BN (*h*-BN), which is the graphite analogue with a layered structure of hexagonal BN units, (ii) cubic BN (*c*-BN), consisting of sp³-hybridized tetrahedral units like in diamond, and (iii) wurtzite BN (*w*-BN), which is also built from sp³-hybridized tetrahedral units, being stacked in a different angle though.[17]
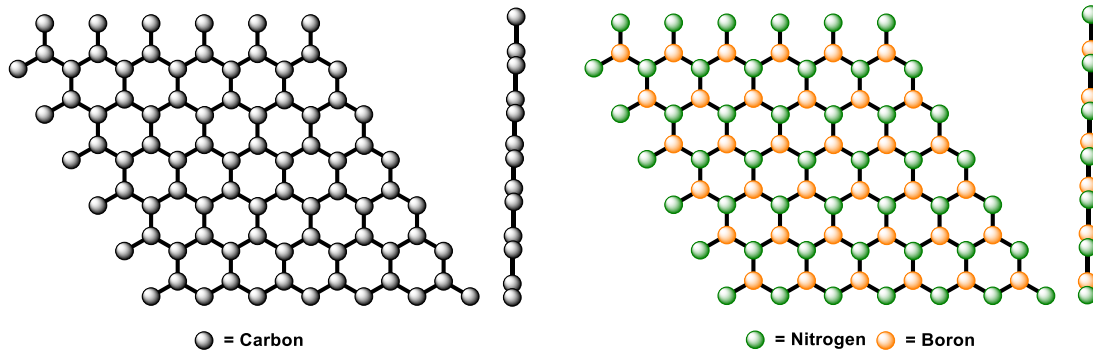
Figure 3: Crystal structures of graphene and boron nitride.

Under standard conditions, *h*-BN is the most stable form owning very good lubricating properties like its graphite counterpart, a very high thermal conductivity and stability, high mechanical strength and high chemical resistance, not being wetted by most molten metals, salts and glasses. Moreover, it is non-toxic and owns a good environmental compatibility. Its limited structural susceptibility for hydrolysis makes it hydrophobic.[18–20]

First synthesized in 1842 by W.H. Balmain from calcium cyanide and boric acid,[21] it took more than a century until Pease proposed the structure of hexagonal boron nitride in 1952.[22] The boron and nitrogen atoms in plane are covalently bound with partially ionic character. The 2D layers are weakly linked by van-der-Waals forces, whereby boron atoms of one plane are in close proximity to a nitrogen atom in another adjacent plane above or below.

The difference in electronegativity of the partners in B-N bonds makes the electron pairs in the sp^2-hybridized σ bonds located mainly on the more electronegative nitrogen atoms. The lone pair in the nitrogen π_z orbital is, in contrast to its graphene analogue, mainly not delocalized to the boron's π_z orbital, resulting in a white color

of the compound. Of high importance for electronic applications is the fact that the binding situation in boron nitride yields a wide bandgap and, consequently, an electrically insulating material (in contrast to graphene) – one important aspect for the use as filler for thermally conductive but electrically insulating polymers. In the case of graphene, the electrons are evenly and equally distributed to all carbon atoms in plane, leading to a dark black color of the substance and a very high electronic conductivity, disqualifying it for the targeted use.

Besides different approaches that yield *h*-BN platelet-shaped particles in large quantities on industrial scale nowadays, mostly using vapor phase synthesis techniques,[12,23–25] the tailoring of substrates on the molecular level adds tremendous advantages to the fabrication of "designer materials" that fit specified needs. This strategy was firstly performed by Poppers and Chantrell[26] in 1964 (Figure 4), paving the path to the so called polymer-derived ceramics (PDCs) route.

In this approach, a molecular precursor (single molecules or polymers) is designed according to the type of ceramic material or the processing route that is needed to shape ceramics in forms of fibers, nanotubes or nano-sheets that are not accessible from commonly used synthetic strategies. The advantages are obvious: properties at the molecular level can be altered easily with the use of organic or inorganic synthesis techniques, yielding substrates that later are transformed by high temperature processes yielding the corresponding ceramics. This route is today mainly used in the preparation of non-oxide ceramics.

Figure 4: General overview about the polymer-derived ceramics route.

In the case of BN ceramics, the use of borazine $B_3N_3H_6$ (BZ) as a carbon-, oxygen- and halogen-free precursor is a well-established practice. There are several advantages to use borazine over other substrates: (i) It is a single-source molecule with a boron to nitrogen ratio of 1:1, offering the same ratio like in BN ceramics. (ii) Its hexagonal planar structure is similar to the structure in the annealed form, rendering a restructuring during pyrolysis unnecessary (Scheme 1). (iii) It is a fluid and, hence, can be relatively easily processed, being volatile at low temperature (boiling point below 60 °C under ambient pressure).[23,27]

Scheme 1: The path from borazine to h-BN.[27]

Despite the abovementioned properties that qualify borazine as a perfect precursor for boron nitride ceramics, complete evaporation in the course of pyrolysis can take

place, which makes the direct synthesis of BN ceramics from borazine hardly feasible. Polymerization of borazine to polyborazines PBZ prior to pyrolysis eliminates this issue and is nowadays a widely used strategy.[28] In 2007, Salles et al. developed a method using a high-frequency nebulized spray generator that vaporizes preliminary tempered borazine into an aerosol that is directly transferred into a pyrolysis furnace at 1400 °C under nitrogen. This technique allows the generation of BN nanoparticles with a size of 55 to 120 nm. X-Ray diffraction analysis of the particles showed the presence of both, an ordered h-BN phase and two disordered boron nitride phases, namely turbostratic BN (t-BN), which consists of hexagonal BN with parts of imperfections, and amorphous BN (a-BN).[23]

2.3 Borazine – a molecular precursor for BN ceramics

Borazine has been discovered by Alfred Stock in 1926 when he heated B_2H_6 in the presence of NH_3 over 180 °C.[29] He noticed that not only borazine was formed: A higher hydrogen evolution than originally expected made him propose that obviously also various nonvolatile, colorless and probably condensed side products had formed, namely polyborazines PBZ. Succeeding its discovery, research in borazine synthesis has led to different possible routes. For its laboratory use, it has been synthesized in various ways. Until 1995, one of the best syntheses in laboratory scale was the preparation of trichloroborazine and its reduction by sodium boron hydride (Scheme 2).

$$3\ BCl_3 + 3\ NH_3 \quad 2,4,6\text{-}Cl_3B_3N_3H_3 + 6\ HCl$$

$$2,4,6\text{-}Cl_3B_3N_3H_3 + 3\ NaBH_4 \quad B_3N_3H_6 + 3\ NaCl + \frac{3}{2}B_2H_6$$
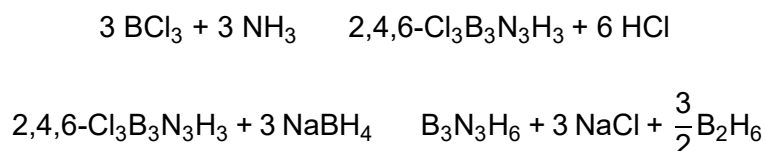
Scheme 2: The formation of borazine using BCl_3 and ammonia.[30]

Sneddon et al. developed a synthesis based on the reaction of ammonium salts such as NH_4Cl, $(NH_4)_2SO_4$, $(NH_4)HSO_4$ and $(NH_4)_2HPO_4$ with sodium borohydride $NaBH_4$ in tetraethylene glycol dimethyl ether $[CH_3(OCH_2CH_2)_4OCH_3$, tetraglyme] that can be performed in solution. The use of NH_4Cl coincided with the formation of chloroborazine, ammonia and acetylene, probably from decomposition of NH_4Cl to NH_3 and HCl leading to various side reactions, excluding NH_4Cl as a proper substrate for the synthesis of borazine. As best-suited alternative substrate, Sneddon et al. identified $(NH_4)_2SO_4$ (Scheme 3) in a molar ratio of $(NH_4)_2SO_4:NaBH_4 = 1:0.65$.[30]

$$3\ NH_{4\ 2}SO_4 + 6\ NaBH_4 \xrightarrow[\text{2-6 mbar}]{\substack{\text{120-140 °C, 3 h} \\ \text{tetraglyme}}} 2\ B_3N_3H_6 + 3\ Na_2SO_4 + 18\ H_2$$
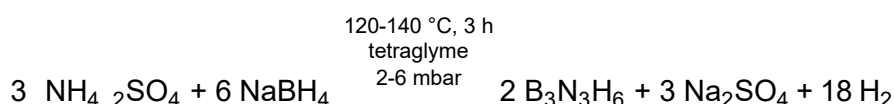
Scheme 3: The formation of borazine using $(NH_4)_2SO_4$ and $NaBH_4$.

Using conditions as described, *"[…] borazine is the only volatile product observed in the reaction, [and can be] obtained in excellent purity even without vacuum fractionation".*[30] It is continuously removed under a dynamic vacuum at 2-6 mbar and collected in a series of cooling traps at −45 °C (for the condensation of tetraglyme), −78 °C (for the condensation of borazine) and −196 °C (for the condensation of other more volatile compounds), yielding 59.9% borazine referred to BH_4^- (Figure 5).[30] It is poorly thermally stable at RT, air- and moisture sensitive and has to be stored in an argon filled glovebox.[31,32]
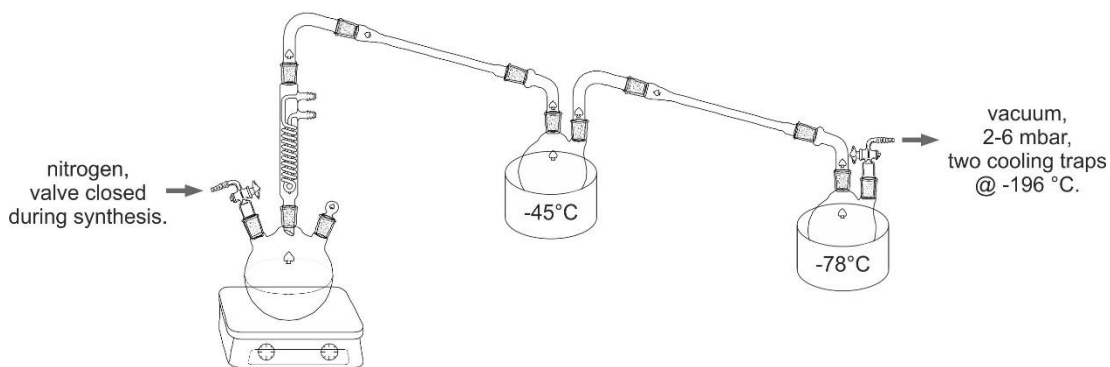
Figure 5: Apparatus used for the synthesis of borazine.

Taking into account that borazine undergoes polymerization reactions from 45 °C onwards,[27] a reaction temperature of 120-140 °C does not favor the product to be formed in high yield. Li et al. studied the use of aluminum chloride as catalyst and showed that the reaction temperature can be significantly lowered to 45 °C and the yield increased to 67%.[33] Observing the reaction via ^{11}B-NMR spectroscopic methods show that small amounts of $Al(BH_4)_3$ are formed, which are expected to play an important role in the formation of borazine (Scheme 4).

$$3\,NaBH_4 + AlCl_3 \rightarrow 3\,NaCl + Al\,BH_4\ _3$$

$$2\,Al\,BH_4\ _3 + 3\ NH_4\ _2SO_4 \rightarrow Al_2\ SO_4\ _3 + 2\,B_3N_3H_6 + 18\,H_2$$

$$Al_2\ SO_4\ _3 + 6\,NaBH_4 \rightarrow 2\,Al\,BH\quad + 3\,Na_2SO_4$$
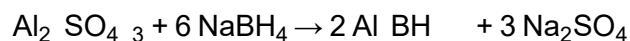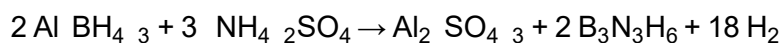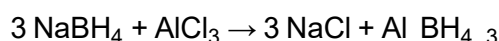
Scheme 4: Proposed reaction pathway for the formation of borazine using AlCl₃ as catalyst.[33]

Besides borazine, additional other products were observed in different amounts by Li et al. (Table 2).

Table 2: Products formed during the synthesis of borazine.

compound	^{11}B NMR shift δ [ppm]	J_{BH} [Hz]	multiplicity
borazine	29.1-30.5[34]	133-139[34]	doublet[34]
cyclotriborazane	-13.5	104	triplet[35]
µ-aminodiborane	-24.8	130[36]	doubletic triplet[36]
ammonia borane	-25.2	91[36]	quartet
sodium boron hydride	-45.2	82	quintet

Those observations were summarized in the proposal of a detailed reaction pathway for the synthesis of borazine from $NaBH_4$ and $(NH_4)_2SO_4$ (Scheme 5).[37]
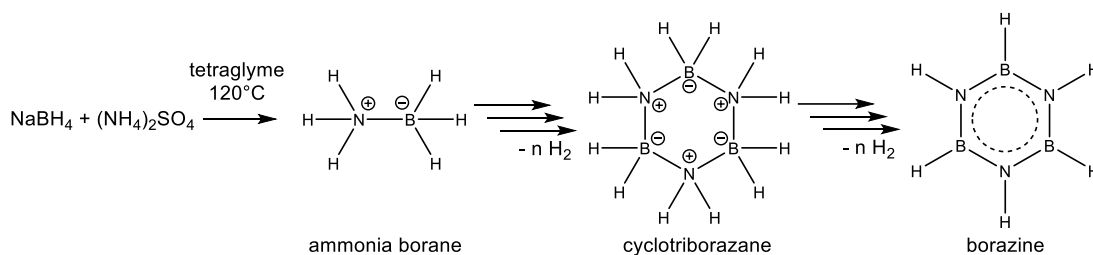
Scheme 5: Proposed reaction pathway to borazine.

µ-aminodiborane is a diborane species, in which one hydrogen is replaced by an amino group. The crystal structures of the [18]-crown-6 adduct and of the THF adduct of this compound have been reported (Figure 6).
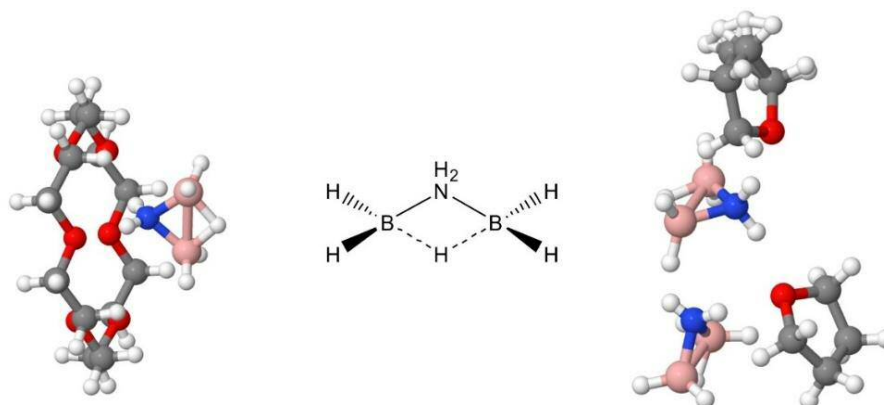
Figure 6: Crystal structures of µ-aminodiborane [18]-crown-6 and THF adducts.[38,39]

2.4 From borazine to BN-ceramics

Starting from borazine, polyborazines can easily be generated from heating under autoclave conditions. Depending on the polymerization conditions, oligomers of different chain length are formed. Miele et al.[27] pointed out that the polymerization parameters such as the molecular weight, the crosslinking degree as well as the hydrogen, boron and nitrogen contents can be controlled by the parameters temperature, time and atmosphere (air, ammonia, argon or nitrogen).

As shown by Sneddon et al. in 1995, polymerization of borazine at 70 °C for 24-48 h under nitrogen atmosphere yields a white polymer in high yields (81-91%) that is soluble in ethers and glymes.[40] The crude polymer can easily be precipitated by adding glyme solutions of the polymer to pentane; the recovered product has an average empirical formula of $B_3N_{3.1}H_{3.4}$.[40] Polyborazines that result of a simple dehydrogenation reaction should have an empirical formula of $B_3N_3H_4$. The lower amount of hydrogen can be explained by condensation reactions that occur during polymerization (Scheme 1).

After its polymerization, PBZ can further be processed by pyrolysis at temperatures between 900 to 1450 °C in inert atmosphere like ammonia, nitrogen or argon, yielding boron nitride of different structures, offering the option for a post-processing annealing to 1800 °C to increase the relative density.[41] The temperature has a great influence on the resulting structure of boron nitride (Figure 7). Broad reflections in recorded XRD spectra that resulted of a lower temperature treatment at 900 °C indicate a less ordered system, whereas a high temperature annealing at 1450 °C leads to sharp reflections that result from a highly ordered hexagonal boron nitride structure.[42]
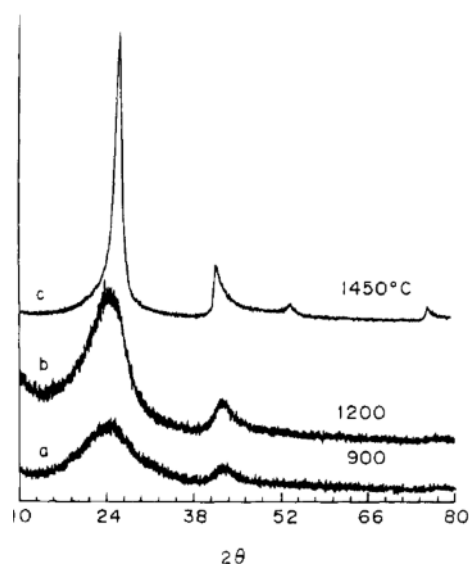
Figure 7: XRD patterns of boron nitride produced from polyborazine under argon at (a) 900, (b) 1200, and (c) 1450 °C.[40]

It is worth mentioning that the ceramic yield depends on the physical state of the substrate. Liquid PBZ has a relatively poor ceramic yield below 55%, in contrast to more than 90% for solid PBZ.[27]

As mentioned before, three different structures of boron nitride exist: (i) hexagonal BN, (ii) cubic BN, and (iii) wurtzite-like BN. Within these classes, different structures are possible. In the case of the most stable modification h-BN, the layers can be stacked in a completely perfect manner, leading to graphite-like boron nitride. Imperfections lead to a less ordered system, in which the structure failures lead to a so called turbostratic structure, where adjacent plane distances are not constant. As third hexagonal modification, an amorphous structure has to be mentioned, where no systematical order exists at all.

2.5 Integration of boron nitride into polymer matrices and possible modifications of the filler material

Although various studies have been published describing the use of boron nitride as filler for high thermal-conductive composites, the weak filler-to-matrix interaction leads to tremendous problems concerning the mechanical performance of polymers and high thermal resistance at the matrix-filler interfaces.[12] In general, there are two different approaches available to minimize those challenges: (i) modifying boron nitride particles with functional groups that increase the van-der-Waals interaction with the matrix, and/or (ii) the preparation of boron nitride nanocomposites, in which the filler is covalently bound to the surrounding matrix through functional groups that allow polymerization reactions to take place directly at the particles. Both strategies require functional units situated at the particles before a modification can occur.[43]

Hexagonal boron nitride consists of platelet-like shapes with a minimal amount of hydroxyl groups in the basal plane (Figure 8). Those OH groups can be modified using electrophilic reagents. The number of reactive sites for functionalization is reasonably low, though, making an enhanced modification necessary.
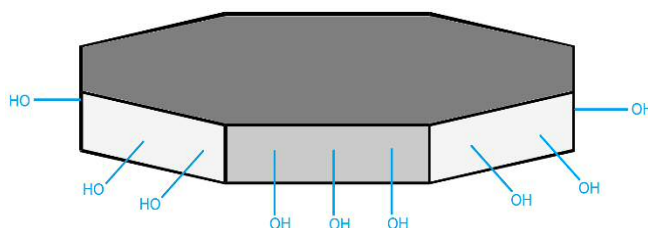
Figure 8: General figure for the structure of h-BN nanoplatelets with -OH functional groups in the basal plane.

A scission of B-N bonds yields reaction sites at both involved atoms, consequently leading to the addition of an even number of functional units. If a functional reactant binds to either boron or nitrogen, another functional group should be added to the counterpart atom to balance the overall charge.[19]

Besides functionalization with alkyl- (-R), alkoxy- (-OR), amino- ($-NH_2$) and amine groups (-NHR), hydroxylation is possible for any electrophilic boron atom in the structure (Figure 9). Those reactions mostly need harsh conditions such as plasma treatment, NaOH-assisted ball milling, treatment with water at 850 °C or peroxide species that can form OH radicals.[19]

In 2011, Lin et al. developed a synthetic strategy based on the sonication of boron nitride powder in deionized water for 8 h, yielding bulk particles in the form of nanosheets of several nm thickness dispersed in the aqueous solutions – both from exfoliation on the one hand and cutting induced by hydrolysis of B-N bonds starting at a nitrogen edged hole defect on the other.[20] Filtration of these dispersions through 0.1 µm pore-sized polycarbonate filter membranes (Millipore Isopore) yielded flexible, ~3 µm thick films of h-BN.

In 2015, Huang et al. described the use of an aqueous 30 wt.-% H_2O_2 solution that was sonicated for several minutes prior to heating to 80 °C for 1 h. Afterwards, the mixture was refluxed at 105 °C for 4 h under vigorous stirring leading to the hydroxylation of BN particles. These BN nanosheets were filtered through a 0.45 µm pore-size filter, washed with water twice and dried under vacuum at 80 °C. They used X-ray photo electron spectroscopy to study the binding situation in the OH-functionalized BN nanosheets and concluded that around 6 wt.-% oxygen was added to the surface of the particles.[43,44] Different approaches to the functionalization of BN nanoparticles are shown in Figure 9.
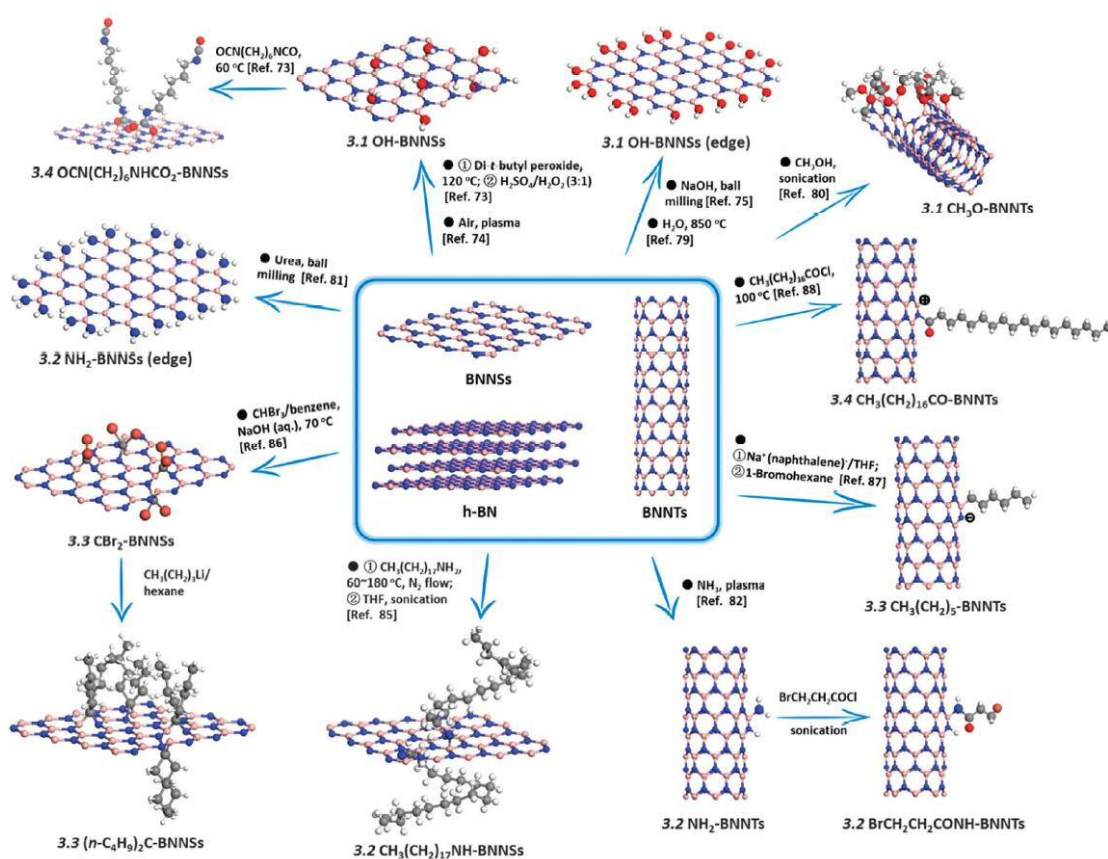
Figure 9: Summary of chemical functionalization strategies of h-BN bulk-/nanomaterials.[19]

A surface containing a significant amount of OH groups can easily be altered using various electrophilic reagents (Scheme 6). Functional units in the backbone of the electrophilic modification agent that are not electrophilic will not react with the hydroxyl groups of the boron nitride surface. Dedicatedly functionalized particles can be covalently bound to the surrounding matrix. For the filling of epoxide resins with boron nitride (in order to enhance the thermal conductivity), the introduction of amine groups (-NH$_2$) is of special interest.
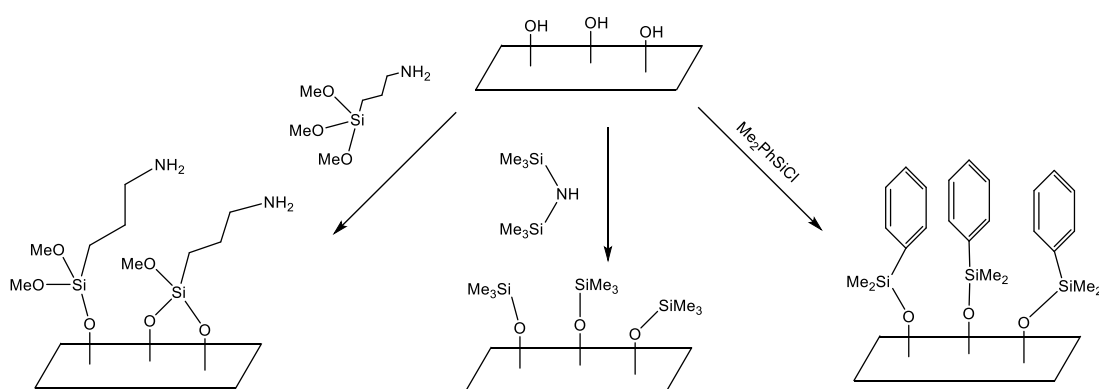
Scheme 6: Various possible modification routes for hydroxyl-functionalized boron nitride particle surfaces.

2.6 Nanocomposites: Enhancing the thermal conductivity with BN nanoparticles

Besides the incorporation of unmodified boron nitride particles into various polymer matrices such as PS, PVB, PMMA, PEVA, PVA, PU, PC, PE and PNIPAM (Figure 10), various reports have been published on the introduction of surface-

modified analogues of boron nitride into epoxy resins.[44–53] In general, it is not only the thermal conductivity, but also the mechanical properties that can be altered by this strategy.

Sainsbury et al. reported the enhancement of 186% of the elastic modulus of PVA with hydroxylated boron nitride nanosheets OH-BNNSs with a load of just 0.1 wt.-% of filler. In comparison, the unmodified particles increased the modulus just around 20% with the same load, verifying that a high interaction of filler to matrix is of high importance.[48]
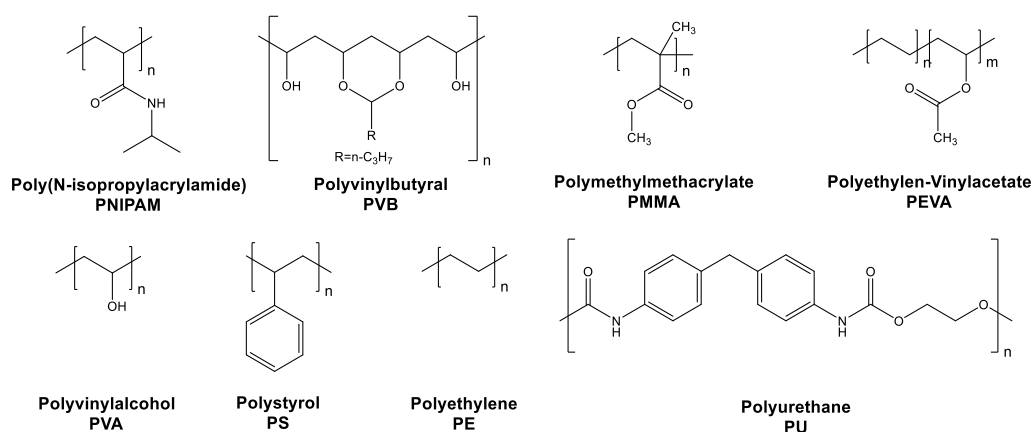
Figure 10: Polymers used to study the mechanical and thermal properties of boron nitride filled matrices.

As boron nitride has a thermal conductivity of approximately 600 W m^{-1} K^{-1} in the basal plane and 30 W m^{-1} K^{-1} perpendicular to it, it has been argued that a self-assembling structure with edge-end-functionalized platelet-shaped particles could probably overcome the issue of strong phonon-scattering and -dispersion at the matrix-filler interfaces and the generation of interconnected thermally conducting

networks.[19] Until now, high contents of boron nitride fillers are commonly needed to improve the thermal conductivity of polymers in a significant manner.

2.7 Epoxide resins with high thermal but low electrical conductivity

Epoxide resins are widely used in various fields of high voltage applications, both as insulating agent and as adhesives. Those resins consist of bi-functionalized aromatic systems (mostly Bisphenol-A; Figure 11) that are terminated with two epoxide groups and can be polymerized with curing agents such as anhydride reagents or amines. As the epoxy resins possess thermal conductivities far below 1 W m^{-1} K^{-1}, their modification with nano-scaled fillers is of great interest.
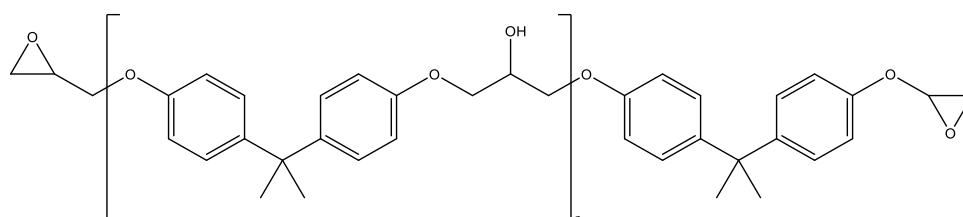
Figure 11: General structure of Bisphenol-A-based epoxy resins with terminal epoxy groups.

Zhi et al. modified boron nitride nanotubes with polyhedral oligosilsesquioxane (POSS) and managed to enhance the thermal conductivity of the epoxy resins to 3 W m^{-1} K^{-1} with a load of 30 wt.-% of filler.[51] Wang et al. increased the thermal conductivity of epoxide resins with a 40 wt.-% fraction of unmodified BN nanosheets to 6 W m^{-1} K^{-1}, corresponding to a 14-fold increase compared to blank epoxy.[52]

The reported high filler contents show that a simple introduction of BN nanoparticles does not necessarily coincide with an increase of the thermal conductivity in a significant manner, but rather highlights the importance of chemical modification prior to the introduction of the fillers into the matrix material. As mentioned by Sun et

al., the exfoliation of commercially acquired h-BN seems to be a crucial step to produce high-performance nanocomposites. They describe the sonication of boron nitride nanoparticles in isopropyl alcohol that led to both, the dispersion and exfoliation of the material, resulting in platelet-like particles with an aspect ratio of 100, a lateral size (edge-to-edge) of more than 1 µm and a thickness of 10-20 nm. The introduction of these particles into a polymer matrix resulted in a high-performance epoxy/BN nanocomposite with a thermal conductivity of 30 W m^{-1} K^{-1}. The highest potential in improving heat transfer values lies in the optimization of exfoliation of boron nitride to few layered sheets in a more controlled way.[54]

2.8 Exfoliation of boron nitride – step for step to 2D structures

Coinciding with the first evidence that carbon nanosheets could relatively easy be obtained by peeling off layer after layer of graphite leading to graphene, additional studies aimed at the application of this method to other compounds such as BN, NbSe$_2$ and MoS$_2$.[55–57] It hast to be emphasized that this process is not feasible for BN, however. The reason could be due to a metastable energy minimum that is reached when the "*number of dangling bonds […] is decreased to a minimum*", making multi-layered boron nitride energetically more stable.[57–59] Since it was shown that mechanical peel off is not very effective for multi-layered structures of BN, another approach was chosen to break up the relatively weak van-der-Waals forces between the layers using gentle shear forces. In 2011, Li et al. used a wet ball-milling process with benzyl benzoate as milling agent under inert nitrogen conditions to generate boron nitride nanosheets (Figure 12).

Besides mechanical exfoliation, different studies were performed using chemicals with different properties. In 2009, Zhi et al. used *N,N*-dimethylformamide (DMF) as strong polar solvent for BN yielding milligram levels of BN nanosheets with heights

between 2 and 10 nm.[61] In 2013, Zhao et al. published a study, in which they used molten sodium hydroxide and potassium hydroxide in a Teflon-lined stainless steel autoclave at 180 °C for 2 h to produce BN nanosheets.[62]
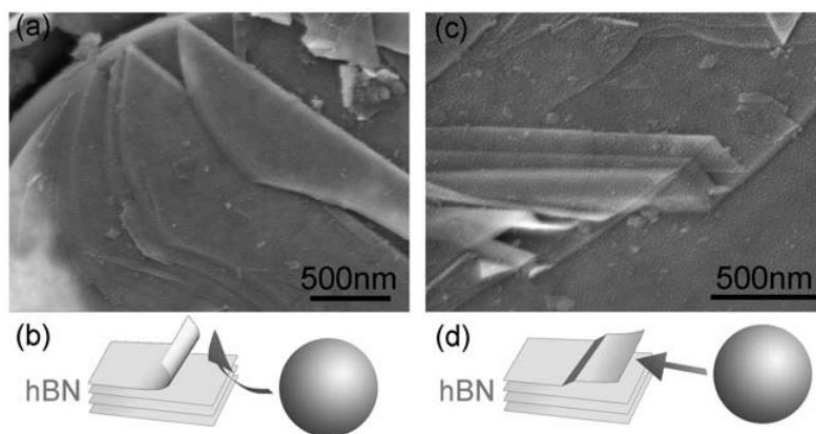
Figure 12: SEM images of treated BN Nanosheets that reveal two possible forces that can occur during a milling process.[60]

Other approaches combine both, chemical and mechanical exfoliation processes, but require more specific equipment. Two of these strategies are known as "high pressure microfludization process" and "vortex fluidic exfoliation". Both techniques make use of boron nitride particles suspended in suitable solvents that are accelerated in a certain manner. Due to collision processes with other particles or equipment surfaces, the exfoliation of boron nitride succeeds (Figure 13).[63,64]
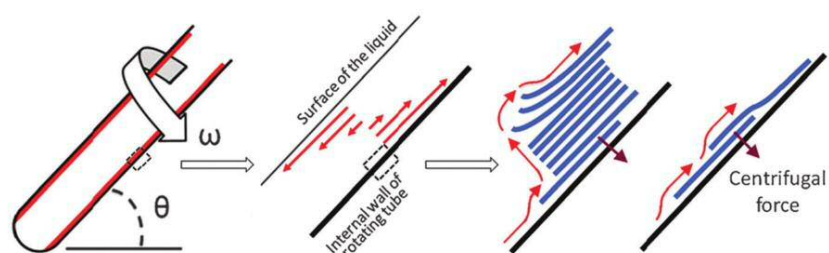
Figure 13: Schematic representation of the exfoliation process taking place during the vortex fluidic exfoliation.[64]

3. Novel Results

3.1 Synthesis of borazine without catalyst

$$3\ (NH_4)_2SO_4 + 6\ NaBH_4 \xrightarrow[\substack{\text{tetraglyme}\\ \text{2-6 mbar}}]{\text{120-140 °C, 3 h}} 2\ B_3N_3H_6 + 3\ Na_2SO_4 + 18\ H_2$$
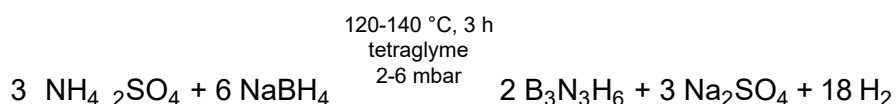
Scheme 7: The formation of borazine using $(NH_4)_2SO_4$ and $NaBH_4$.

Miele et al. reported that the synthesis of borazine can be easily performed with chemicals "used as received", yielding borazine in "excellent purity without further purification" (Figure 5).[23,31] The synthetic route described in their study, however, could not be reproduced successfully: Foaming during the synthesis as well as the recovery of white solid compounds (instead of a colorless liquid) revealed the need of modification of both, reactants and apparatus. In 1998, Wideman et al. also addressed the synthetic conditions for borazine.[65] They emphasized the importance of drying and purification of the solvent tetraglyme (since borazine is prone to hydrolysis) by distillation from molten sodium.

Aiming at safe working conditions, molecular sieves 3A with a pore sizes of 3 Å were chosen as drying agents in this study, reducing the water content of tetraglyme from 100 to 20 ppm (according to Karl-Fisher titrations). A crucial step for the final success of the borazine synthesis was to remove all volatile parts from the solvent using a high dynamic vacuum at <1 mbar and degas it for several hours. These purification steps together with the modification of the apparatus (such that the reaction mixture could be stirred at atmospheric pressure for the first hour of

reaction, using a bubbler connected to the nitrogen source and the valve located at the reaction vessel) minimized foaming to an acceptable level.

A reaction temperature of 80 °C was set for the first hour and was continuously raised to 135 °C afterwards. That temperature was held for 3 h. The condensation of reactants at reduced pressure using a rotary oil pump after one hour of reaction yielded tetraglyme at −40 to −50 °C, borazine as clear liquid at −78 °C, and other volatile compounds such as oligomeric amino borane ($[BH_2NH_2]_n$) at −196 °C.

^{1}H-NMR spectroscopic measurements of the 'borazine charge' (the reactants that were collected at −78 °C) showed the presence of around 20% of an additional substance besides borazine (Figure 14). Borazine itself is represented by to multiplets at δ = 5.5 ppm (N**H**) and δ = 4.4 ppm (B**H**) of identical integral size.
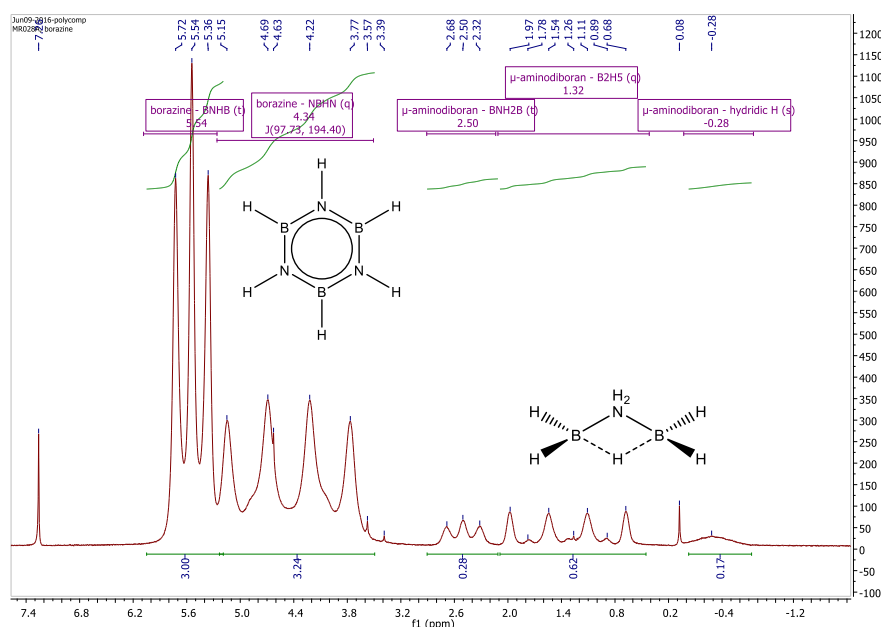
Figure 14: ^{1}H-NMR spectrum of borazine and µ-aminodiborane received by condensation at −78 °C, preceded by synthesis at 135 °C for 3 h at <5 mbar.

The additional compound was identified as μ-aminodiborane (Scheme 7) using ^{11}B-NMR spectroscopic methods (Figure 15). μ-aminodiborane consists of two borane units that are linked *via* an amino group instead of a bridging hydrogen atom.[66]

diborane   μ-aminodiborane

Scheme 8: Structures of diborane and μ-aminodiborane.

In 1964, Schaeffer and Gaines studied some μ-aminodiboranes and amine boranes using a Varian Modell 4300B high resolution spectrometer at a frequency of 19.3 MHz[36] and published spectra and coupling constants that are consistent with our received spectra at a frequency of 500 MHz (Figure 15, Table 3).
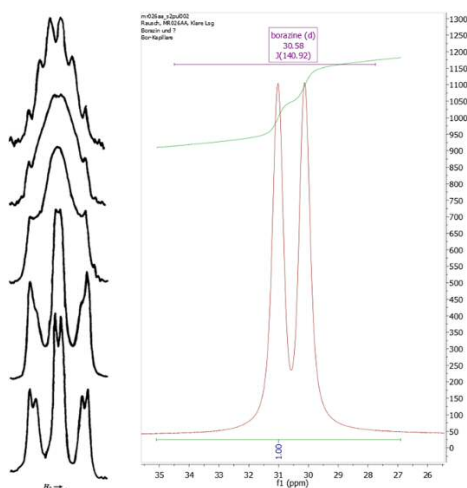
Figure 15: Left: ^{11}B-NMR spectra from Gaines and Schaeffer published in 1964; the spectra were recorded at (from bottom to top) −39, −6, 42, 63 and 83 °C. **Right:** ^{11}B-NMR spectrum at room temperature (own findings).

Table 3: Chemical shifts and coupling constants derived from ^{11}B-NMR spectra of µ-aminodiborane.

	δ [ppm]	J^1 BH₂ [Hz]	J^2 BHB [Hz]
Schaeffer/Gaines, 1963	-26.7	130 ± 2	30 ± 2
Kaschnitz/Rausch, 2016	-26.52	131.14	33.52

^{1}H-NMR studies (Figure 16) further proofed the presence of µ-aminodiborane: Boron mainly consists of a mixture of [10]B (spin: 3) and [11]B isotopes (spin: 3/2) in a ratio of 19.9% and 80.1%, respectively; the B**H₂** protons are represented by a multiplet in the shape of a tripletic quadruplet at δ = 1.25 ppm, in which the weak tripletic resonances can be associated to the coupling of the protons with [10]B. The protons at the nitrogen atom N**H₂** are represented by the triplet at δ = 2.43 ppm. Of great interest is the multiplet resonance at −0.36 ppm: The broadened peak is the result of an exchange reaction of the bridging hydride atom (Scheme 9).
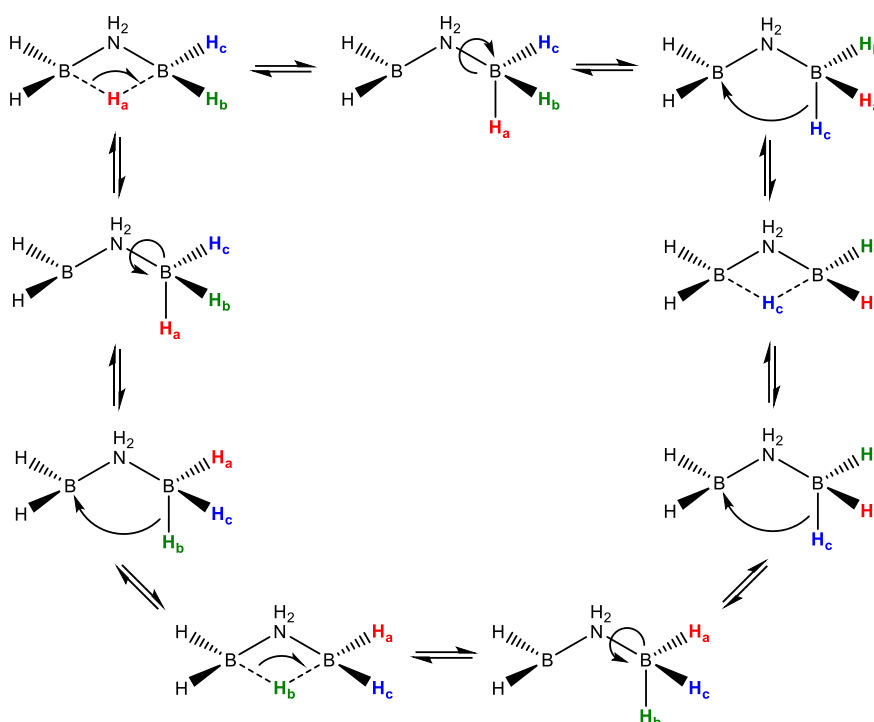
Scheme 9: Proposed hydride exchange reaction of the proton of µ-aminodiborane that leads to a broadening of the resonance at −0.36 ppm in ^{1}H-NMR spectra.

In the case of μ-aminodiborane, the high number of different possible tautomeric forms of the molecule and the velocity of the exchange reaction lead to an overlap of the different corresponding signals and to the massive broadening of the signal for the hydrogen atom (Figure 16). Borazine was as well characterized by ATR-IR spectroscopy, revealing perfect agreement with literature data (Figure 17).
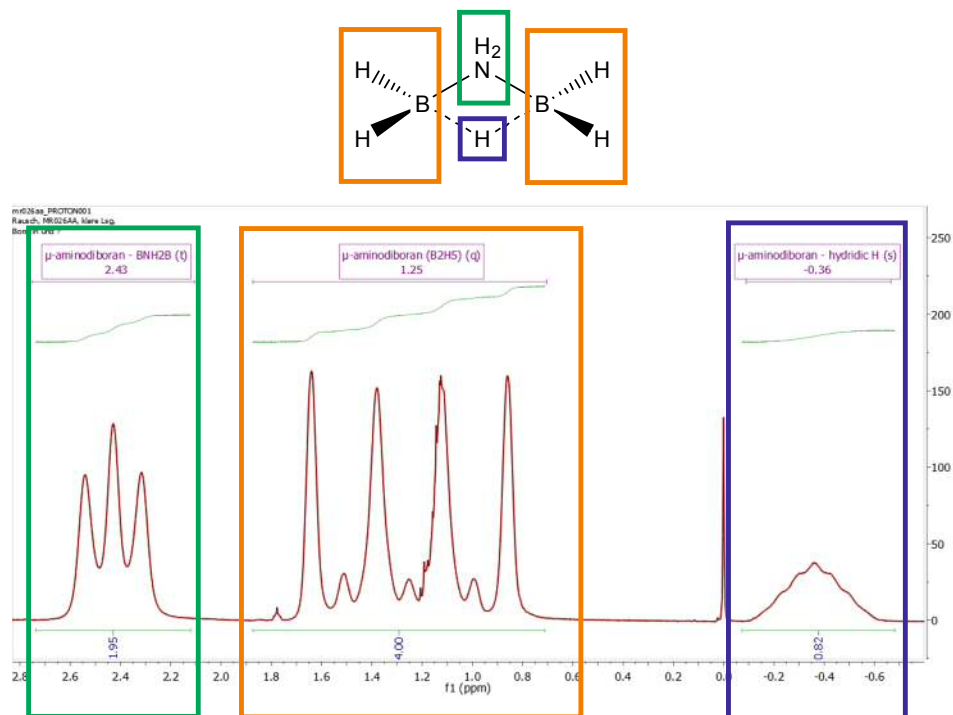
Figure 16: Excerpt of the ^{1}H-NMR spectra (cp. Figure 14) of μ-aminodiborane.
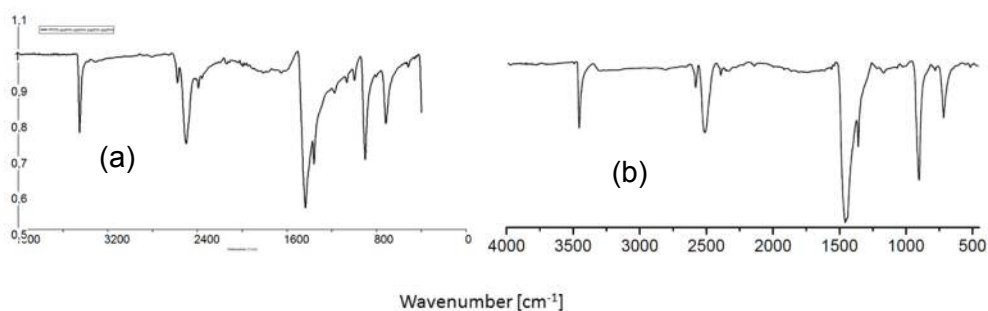
Figure 17: ATR-IR spectra of borazine: (a) recorded spectrum (b) published spectrum by Miele et al.[31]

3.2 Synthesis of borazine with the use of 1 mol% AlCl$_3$ as catalyst

$$3 \ (NH_4)_2SO_4 + 6 \ NaBH_4 \xrightarrow[\substack{\text{tetraglyme} \\ \text{reduced pressure} \\ \text{1 mol\% AlCl}_3}]{\text{45 °C, 3 h}} 2 \ B_3N_3H_6 + 3 \ Na_2SO_4 + 18 \ H_2$$
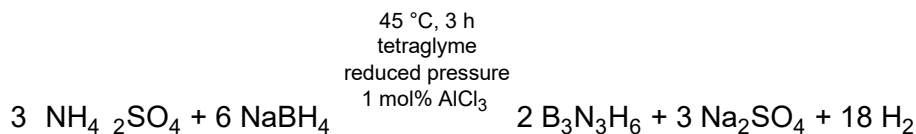
Scheme 10: The formation of borazine using (NH$_4$)$_2$SO$_4$ and NaBH$_4$.

Li et al. described the use of AlCl$_3$ as catalyst for the synthesis of borazine at a reaction temperature of 45 °C.[33] During reproduction it was found, in contrast to Li's conditions, that the isolation of borazine *via* condensation was successful only after the reaction mixture had been stirred at 45 °C under atmospheric pressure for 48 h and not, as they mentioned, *via* continuous condensation. Borazine could not be obtained in perfectly pure yield (Figure 18); again, μ-aminodiborane was formed (approx. 5%). μ-aminodiborane was also recovered when the reaction was carried out at a temperature of 100 °C with AlCl$_3$ as catalyst – however, in an exceeded ratio of borazine to μ-aminodiborane of 2:1 (Figure 19).

In contrast to the report by Li et al., the synthesis of borazine using AlCl$_3$ as catalyst did not lead to any "improved yield [of borazine]"[33], but even decreased the yield. Although a small amount of borazine could be recovered and characterized using ^{1}H- and ^{11}B-NMR spectroscopic methods (proton coupled and decoupled; Figure 18; Figure 19; Figure 20), no improvement at all could be achieved using AlCl$_3$ as catalyst. One possible reason could be the necessity of distilling the solvent from molten sodium prior to use to decrease to water content to a value smaller 20 ppm, what was not performed because of the above described safety considerations.
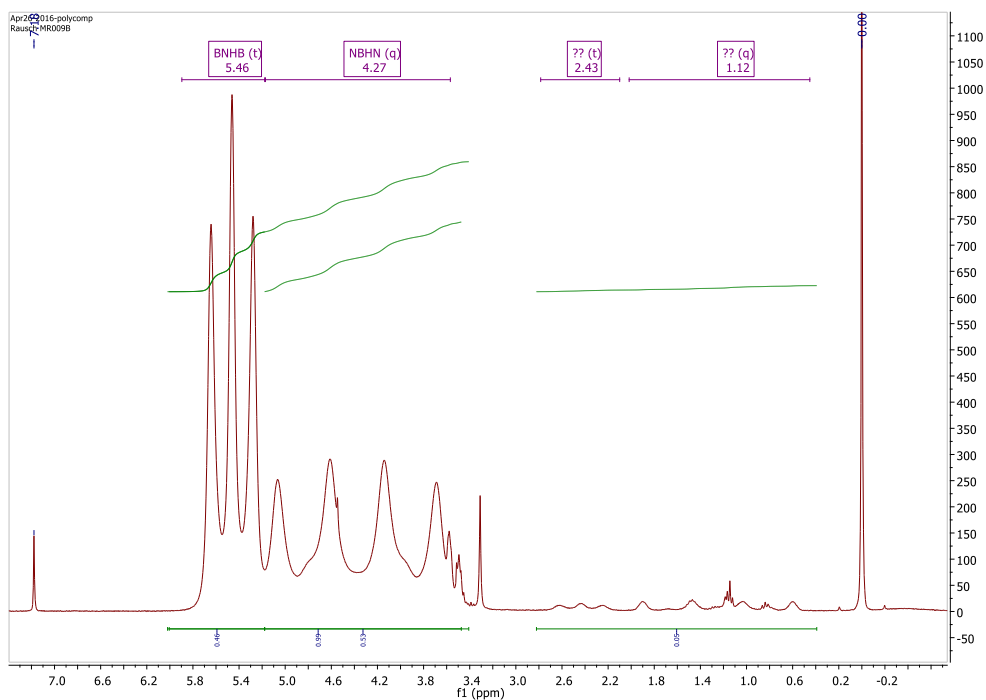
Figure 18: ^{1}H-NMR spectrum of borazine, synthesized at 45 °C for 48 h under atmospheric pressure using 1 mol% AlCl$_3$ (in reference to NaBH$_4$) as catalyst.
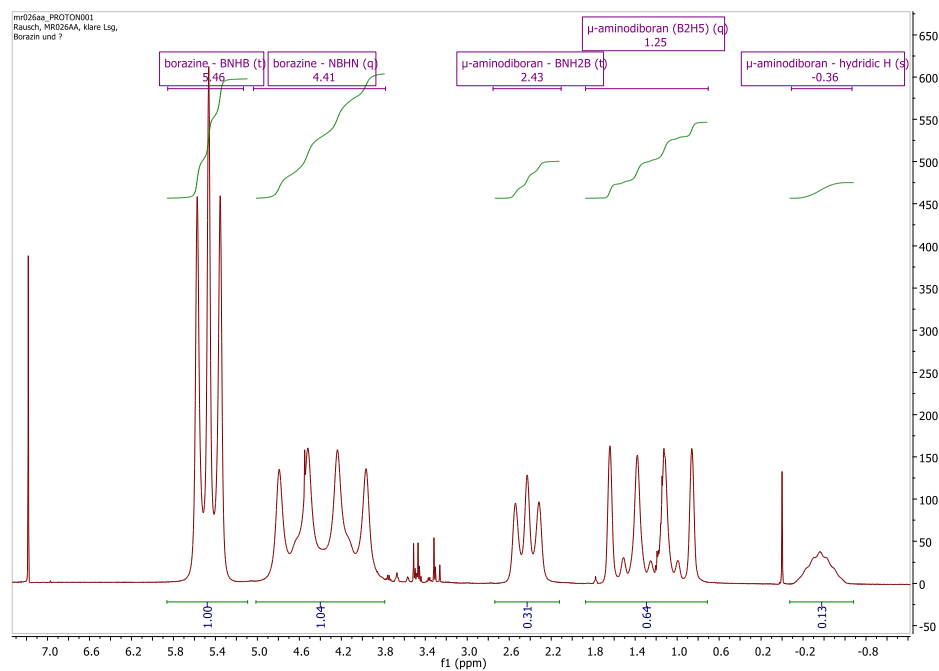
Figure 19: ^{1}H-NMR spectrum of borazine and µ-aminodiboran received by condensation at −196 °C, synthesized at 100 °C for 3 h at <1 mbar using 1 mol% AlCl$_3$ (in reference to NaBH$_4$) as catalyst.
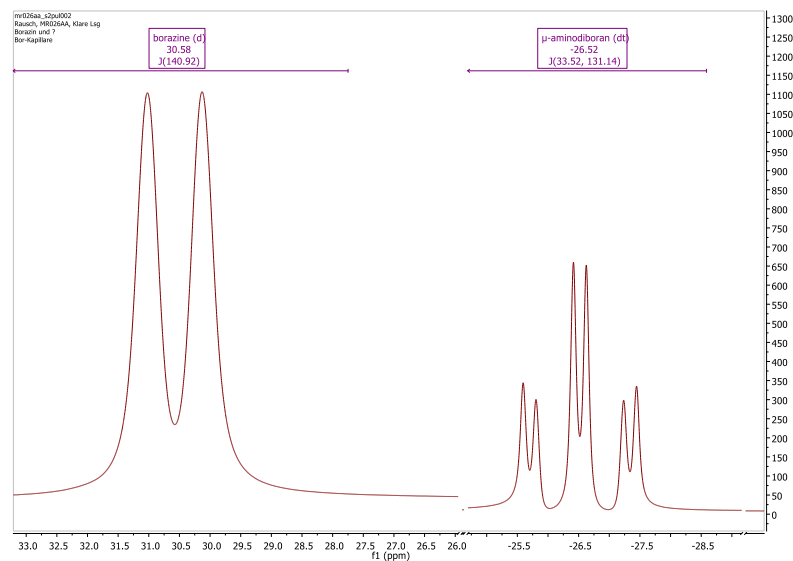
Figure 20: ^{11}B NMR spectrum of borazine and μ-aminodiboran received via condensation at -196 °C, synthesized at 100 °C for 3 h at <1 mbar using 1 mol% AlCl₃ as catalyst.

3.3 Synthesis of polyborazine

borazine   polyborazines of different structure
                                    and chain length
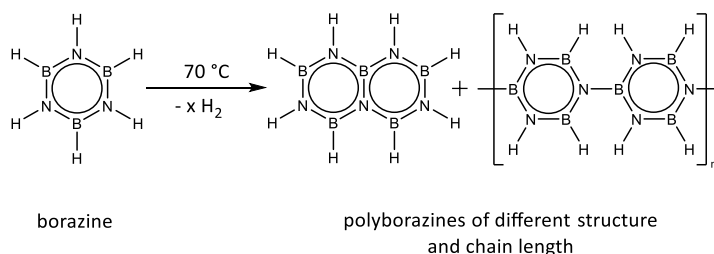
Scheme 11: The formation of polyborazines from borazine.

Since borazine is usually polymerized to polyborazine *in-situ* under autoclave conditions at temperatures from 50 to 70 °C,[27] a preliminary test using the Biotage Initiator chemistry microwave reactor was performed. In this approach, dry $(NH_4)_2SO_4$ and $NaBH_4$ were stirred in tetraglyme abs. in a microwave reaction vial in

the same ratio like in the abovementioned syntheses (chapter 3.1). Due to the sealed microwave reaction vial and the vigorous hydrogen evolution during the reaction, the internal pressure increased and the vial exploded.

Hence, an alternative approach for the polymerization of borazine pointed out by Sneddon and Remsen in 1995 was chosen.[40] As apparatus, a cryostatically cooled reflux condenser was set to 10 °C and the round-bottom reaction vessel was kept at 70 °C for 48 h. After 48 h, all remaining volatile parts were removed under dynamic vacuum, revealing a white gel-like residue that was dissolved in tetraglyme and precipitated in dry pentane. The white flocks were filtrated at ambient conditions using a porous frit, where the residence time at air was kept at a minimum. All volatile parts were removed at a dynamic vacuum in order to dry the polymer. The ATR-IR spectrum revealed the presence of polyborazine (Figure 21). In addition to infrared characterization, the ^{11}B-NMR spectrum showed a broad peak at δ = 20.48 ppm that corresponds to polyborazine as well.
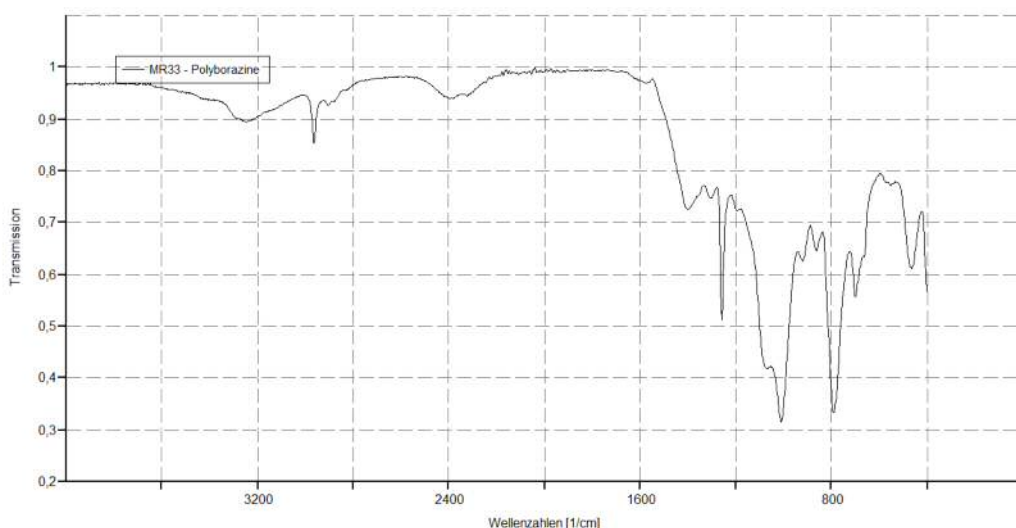
Figure 21: ATR-IR spectrum of polyborazine.

3.4 Pyrolysis of polyborazine yielding boron nitride

Solid polyborazine was transferred to a Netzsch STA 409 C/CD TG/DTA machine and pyrolyzed at 1400 °C with a heating rate of 5 K min^{-1} under nitrogen inert gas with a gas flow of 40 mL min^{-1} and a holding time of 3 h at the maximum temperature. As sample holder, an Al$_2$O$_3$ crucible was used (Figure 22). Weighing of the crucible manually after the pyrolysis finished showed a weight drop of 1.5%.
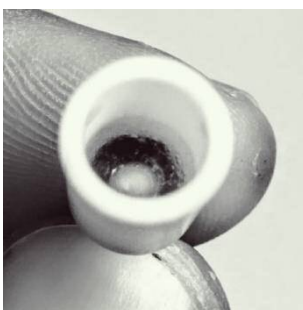
Figure 22: Al$_2$O$_3$ crucible with the clear residue (boron nitride).

The resulting clear solid residue is very brittle and cannot be scratched with a spatula effectively. The ATR-IR spectrum (Figure 23) verifies the successful synthesis of boron nitride.
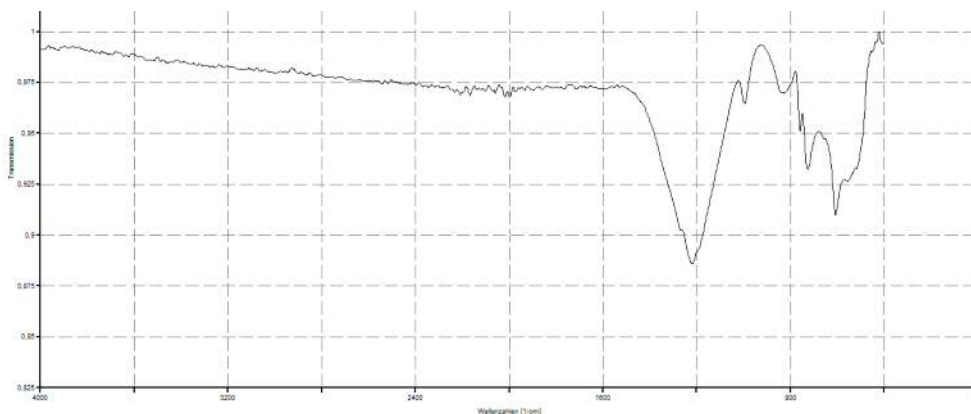
Figure 23: ATR-IR spectrum of BN that was pyrolyzed at 1400 °C.

Light microscopic investigations revealed the presence of a mesoporous structure (Figure 24) that obviously could be the result of vigorous hydrogen gas evolution during the pyrolysis, which lead to cavities in the sub-micrometer regime.
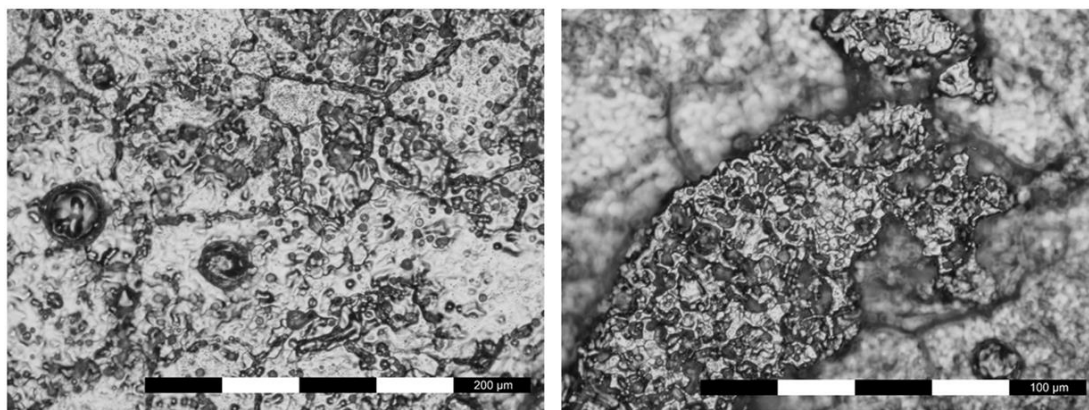
Figure 24: Light microscope picture of mesoporous boron nitride synthesized via the polymer-derived ceramics route.

3.5 Characterization of commercially available boron nitride

Since a large-scale production of boron nitride was not among the aims of this work and the equipment for a spray pyrolysis as described by Miele *et al.* in 2009[23] was not available, boron nitride powder with a mean diameter of 70 nm was purchased from MKnano from Mississauga, Canada. It was characterized using ATR-IR, DLS, XPS and SEM/EDX measurements. The results are outlined below, revealing that the actual particle size was nearly double the size that was stated by the company.

3.5.1 Dynamic light scattering

DLS measurements were performed in order to determine the radii of the particles (Figure 25). The hydrodynamic radii of the supplied particles were 133 nm for a

0.01 wt.-% solution and 208 nm for a 0.05 wt.-% solution of the particles in ethanol (other than the 70 nm stated by the supplier).
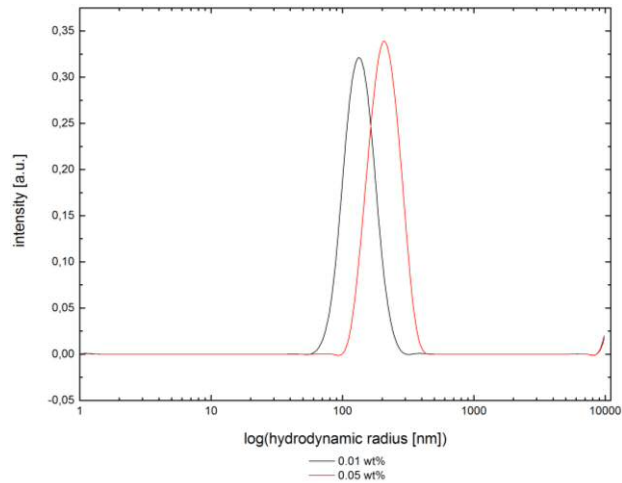
Figure 25: Dynamic light scattering data of crude 70 nm h-BN particles as supplied by MKnano.

Since dynamic light scattering measurements are based on the diffusion of perfectly spherical particles in a Newtonian fluid and their diameter can be expressed using the Stokes-Einstein-equation pointed out in equation (1), measurements of particles that do not possess a perfectly spherical appearance lead to measures that usually are smaller than their effective radius.

$$D = \frac{k_B \cdot T}{6 \cdot \pi \cdot \eta \cdot R_0} \qquad (1)$$

D…diffusion constant
k… Boltzmann constant $1.38 \cdot 10^{-23}$ $J \cdot K^{-1}$
T… temperature K
η…dynamic viscosity of solvent $N \cdot s \cdot m^{-2}$
R_0…hydrodynamic radius of particles [m]

3.5.2 Scanning electron microscopy

SEM/EDX measurements of the BN particles revealed a mean particle size of 137 ± 25 nm (Table 4; in good agreement with the DLS results). The particles had the form of spheres to platelets. They tend to agglomerate (Figure 26), although their preparation on silicon wafers via spin-coating of the corresponding 0.1 wt.-% solution with subsequent drying at 60 °C should have favored the even distribution of the particles throughout the whole wafer.
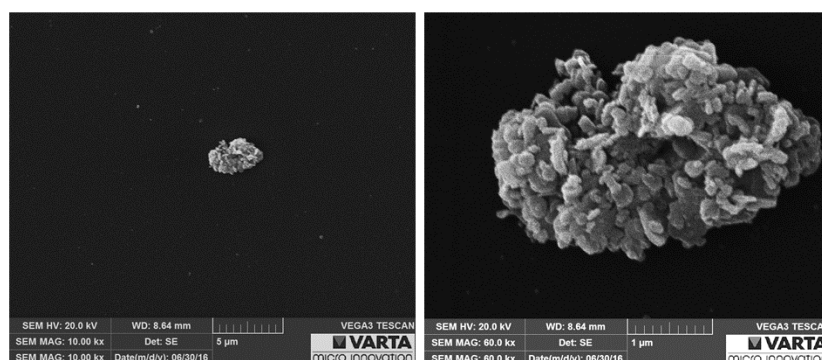
Figure 26: SEM pictures of boron nitride particles supplied by MKnano.

Table 4: Radii and diameters of BN particles measured by SEM/EDX.

Object number	r [nm]	d [nm]	Object number	r [nm]	d [nm]
1	44.73	89.47	15	66.25	132.50
2	48.93	97.85	16	66.59	133.17
3	49.88	99.75	17	73.23	146.46
4	56.08	112.17	18	74.83	149.67
5	56.62	113.25	19	75.02	150.04
6	57.21	114.41	20	77.02	154.04
7	57.64	115.28	21	78.83	157.65
8	59.94	119.89	22	79.04	158.07
9	60.45	120.90	23	81.07	162.15
10	61.04	122.08	24	81.62	163.23
11	62.07	124.15	25	82.29	164.58
12	62.74	125.48	26	85.49	170.98
13	63.18	126.35	27	91.82	183.63
14	65.03	130.06	28	95.10	190.20
mean value				68 ± 13	137 ± 26

3.5.3 Attenuated total reflection – infrared spectroscopy

The boron nitride was of perfect purity, showing the characteristic IR spectrum with a broad peak at 1364 cm^{-1} that can be assigned to the in plane B-N stretching movement and a sharper peak at 777 cm^{-1} corresponding to the out-of-plane bending movement of the B-N bonds (Figure 27).[67] The absence of any OH resonance has to be mentioned.
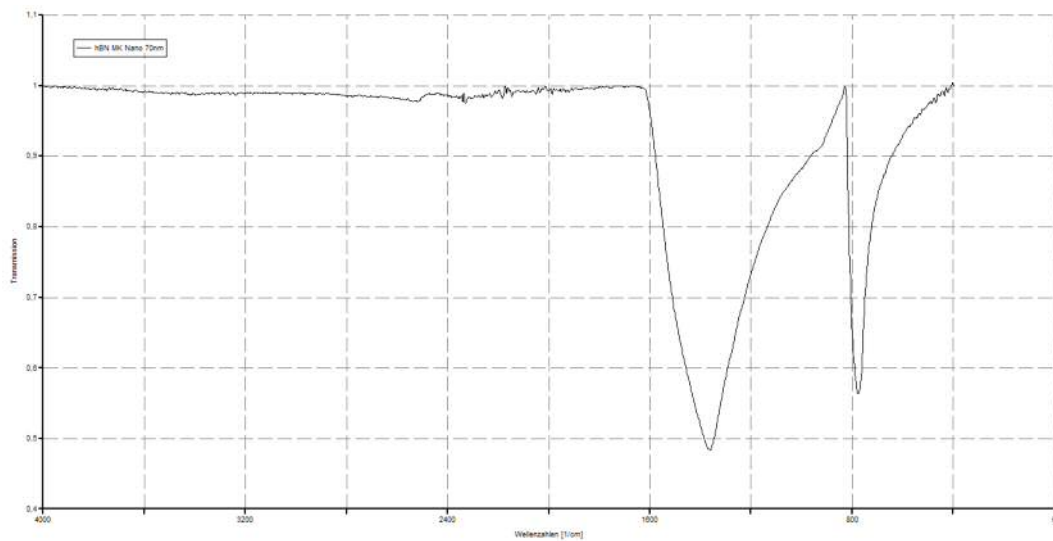
Figure 27: ATR-IR spectrum of boron nitride 70 nm supplied by MKnano.

3.6 Boron nitride activation and modification

For enhanced compatibility of the BN particles in epoxide resins, the modification and activation of the surface of the particles may be considered. In this study, two different approaches were chosen, namely the treatment of the particles with (i) H_2SO_4 and HNO_3 in a ratio of 1:3 as well as (ii) H_2SO_4 and H_2O_2 in a ratio of 2:1 (piranha solution). Both reaction mixtures were sonicated for 6 h at 60 °C and afterwards heated to 80 °C under vigorous stirring for 72 h. After the completion of

the reaction, the opaque solution was centrifuged and the resulting white residue was washed with deionized water until the supernatant was pH-neutral.

3.6.1 Attenuated total reflection – infrared spectroscopy

Although harsh reaction conditions were chosen for the experiments with nitration acid, modification of the boron nitride was not observed in contrast to reported results by Qu et al.[12] (Figure 28), showing that boron nitride is inert against this oxidizing acid. In the case of piranha solution, the resulting white solid residue showed an additional broad peak at 3200 cm^{-1} (Figure 28), corresponding to OH stretching vibration and resonances at 1200, 1050 and 890 cm^{-1} that can be assigned to H_3BO_3 and to B-OH vibrations in general.[50] Hence, piranha solutions can be used for the oxidization of BN, yielding B-OH groups as reactive sites for future modifications.
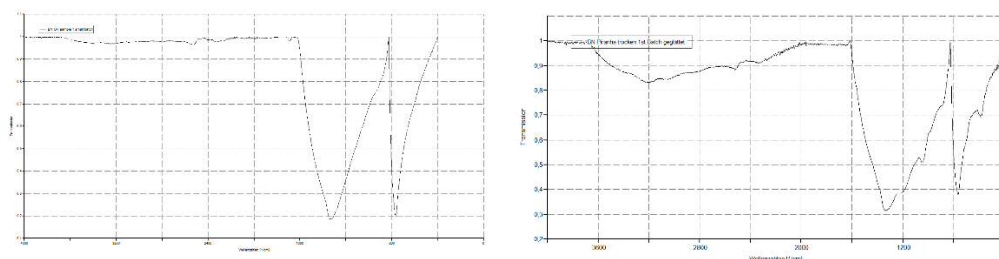
Figure 28: ATR-IR spectra of boron nitride treated with nitration acid (left) and piranha solution (right) for 72 h at 80 °C after sonication at 60 °C for 6 h.

3.6.2 Dynamic light scattering

DLS measurements of particles oxidized by piranha solution were performed in ethanol and revealed a mean particle size of 271 nm for 0.01 wt.-% and 463 nm for 0.05 wt.-% solutions (Figure 29). In comparison to the pristine BN that showed a

particle size of 133 nm for a 0.01 wt.-% solution and 208 nm for a 0.05 wt.-% solution, the increased sizes again are likely to be attributed to the Stokes-Einstein-equation (1) that is based on ideal spherical particles. While the particles were exfoliated under these harsh conditions, the aspect ratio could have changed in a manner that led to the drastic increase of the hydrodynamic radius.
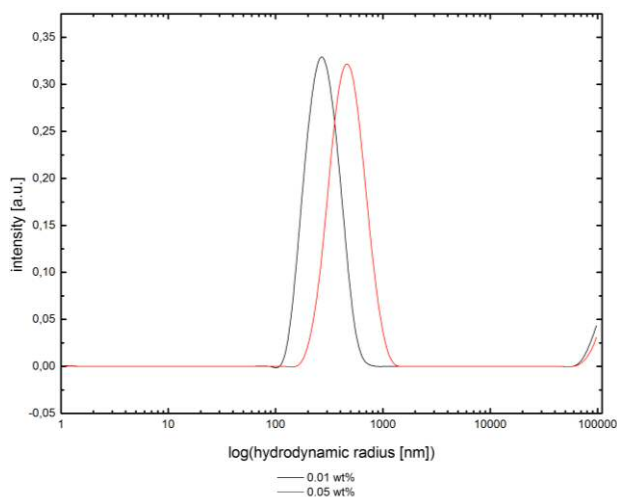
Figure 29: Dynamic light scattering data of boron nitride treated with piranha acid for 80 h.

3.6.3 Scanning electron microscopy

SEM investigations of a 0.01 wt.-% emulsion of piranha acid-treated BN particles in ethanol that was spincast on a silicon wafer and dried revealed the presence of more platelet-like structures compared to pristine BN (Figure 30), evidencing an exfoliation process that took place during the acid treatment. Of special interest is the increase of the effective particle size compared with pristine BN: It increased from 137 ± 25 to 203 ± 130 nm. This effect could be due to pristine particles that were too big to be transferred to the spin coater initially (because of fast sedimentation processes), but were broken up to smaller fragments during the hydrolysis - finally leading to an increase of the average particle size.
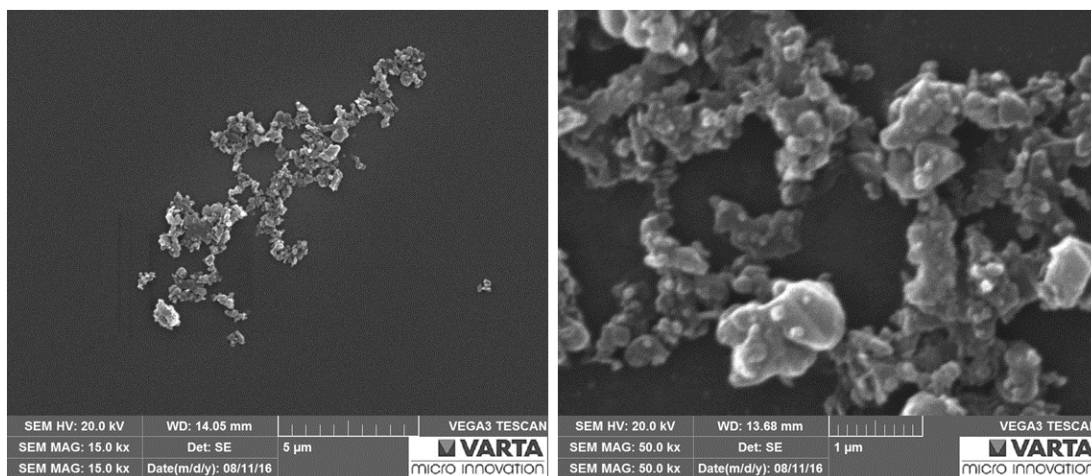
Figure 30: SEM pictures of piranha-acid treated BN nanoparticles.

Table 5: Radii and diameters of piranha acid-treated BN particles measured via SEM/EDX.

Object number	r [nm]	d [nm]	Object number	r [nm]	d [nm]
1	60.65	121.29	12	88.49	176.99
2	64.08	128.17	13	90.44	180.88
3	66.39	132.77	14	91.47	182.93
4	68.05	136.10	15	92.01	184.01
5	69.10	138.20	16	96.95	193.91
6	70.90	141.79	17	98.76	197.53
7	76.11	152.23	18	99.67	199.34
8	78.27	156.55	19	118.91	237.81
9	86.00	172.00	20	119.47	238.93
10	86.77	173.55	21	140.75	281.51
11	87.56	175.12	22	385.68	771.36
mean value				102 ± 65	203 ± 130

3.6.4 X-ray Photoelectron spectroscopy

XPS spectra were recorded on a Thermo Scientific K-Alpha+ X-ray Photoelectron Spectrometer System and processed with Thermo Scientific Avantage Software for surface analysis. The analysis of the piranha-acid treated particles shows both, a

change in the chemical environment of boron and nitrogen as well as a raise in the overall oxygen content, in comparison to the unmodified boron nitride powder (Figure 31).
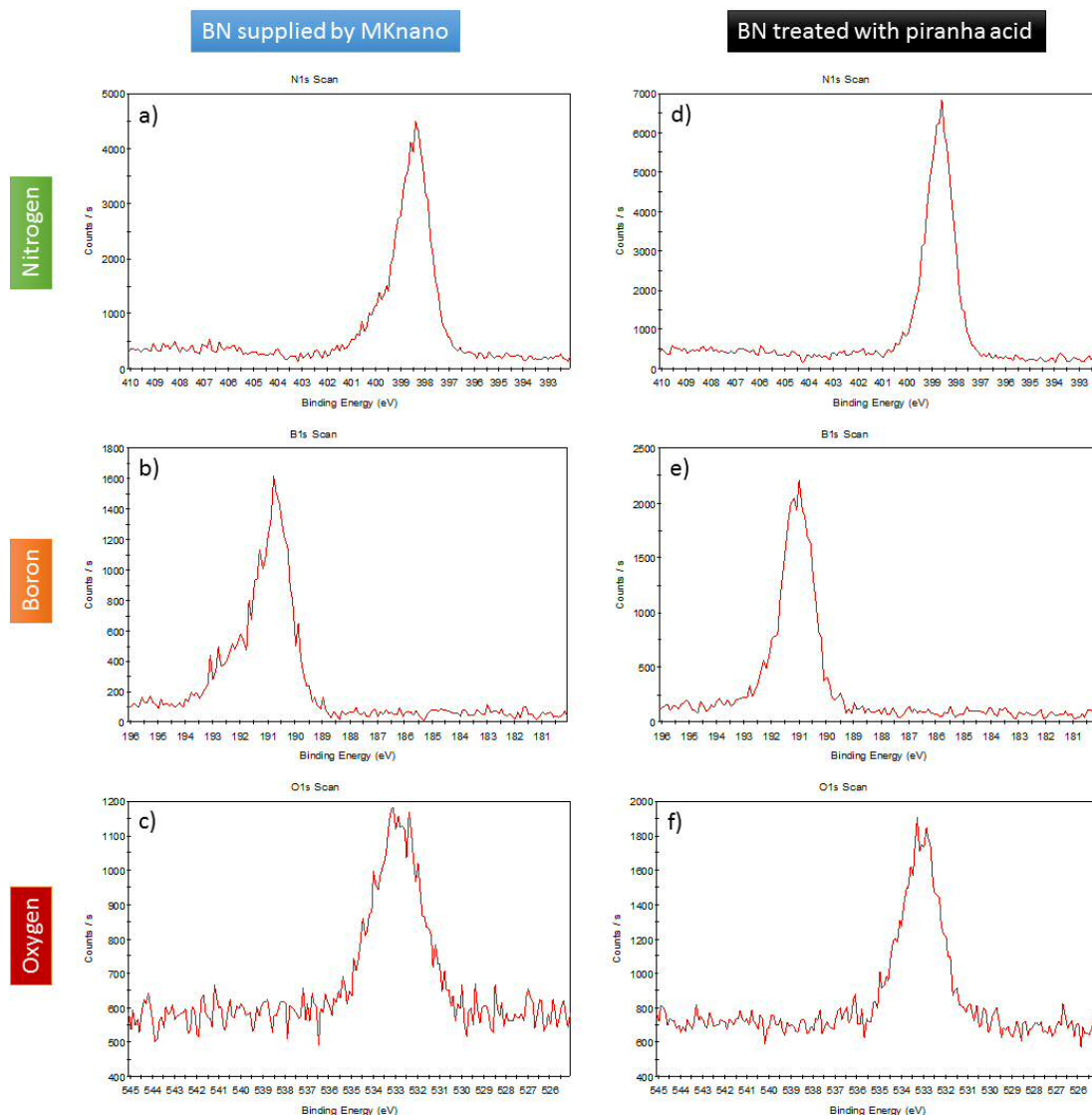
Figure 31: XPS spectra of pristine unmodified BN supplied by MKnano (a-c) and BN treated with piranha acid (d-f).

The treatment of boron nitride with piranha solution leads to a more defined surface (Figure 31). This can be recognized by the higher symmetry of the peaks d, e, and f (compared to a, b, and c). As visible in a, a slight shoulder lies beneath the main

peak of nitrogen, revealing a different chemical ambience for a certain amount of nitrogen. Analogously, a slight shoulder is visible in picture b, indicating the same difference in surrounding for parts of the material. To determine the exact amount and quality of the different chemical environments, a Gaussian fit would be needed, that would approximate curves for each environment. The complete area of the peaks was used to calculate the exact atom percentages of nitrogen, oxygen and boron, revealing a rise of 4.0% of the oxygen atoms during the piranha acid treatment. The functionalization takes place mainly at the boron atoms, in best agreement with proposed reaction sites by Golberg *et al.* in 2016.[19]

Table 6: XPS data of pristine and piranha acid treated BN.

Name	BN supplied by MKnano Atomic %	BN treated with piranha acid Atomic %	absolute change
N1s	46.0	44.8	-1.2
O1s	7.2	11.3	+4.0
B1s	46.8	43.9	-2.8

3.7 Epoxide resin sample preparation and characterization

As epoxide resin system, the combination Araldite CY225 / Aradur HY925 from Huntsman Corp. was chosen. This combination consists of three different parts (Figure 32): (i) the CY225 resin consisting of a diglycidyl ether of bisphenol A, (ii) the HY925 hardener consisting of tetrahydromethyl-1,3-isobenzofurandione (a cyclic anhydride that crosslinks the polymer), and (iii) a quaternary ammonium halide salt that is part of the resin.[68]
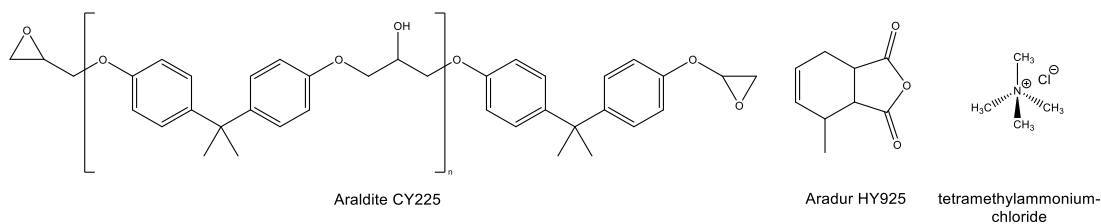
Figure 32: Structures of used accelerated resin / hardener system.

The catalysis by ammonium salts has been argued to address the ring-opening of the cyclic anhydrides (Scheme 12).
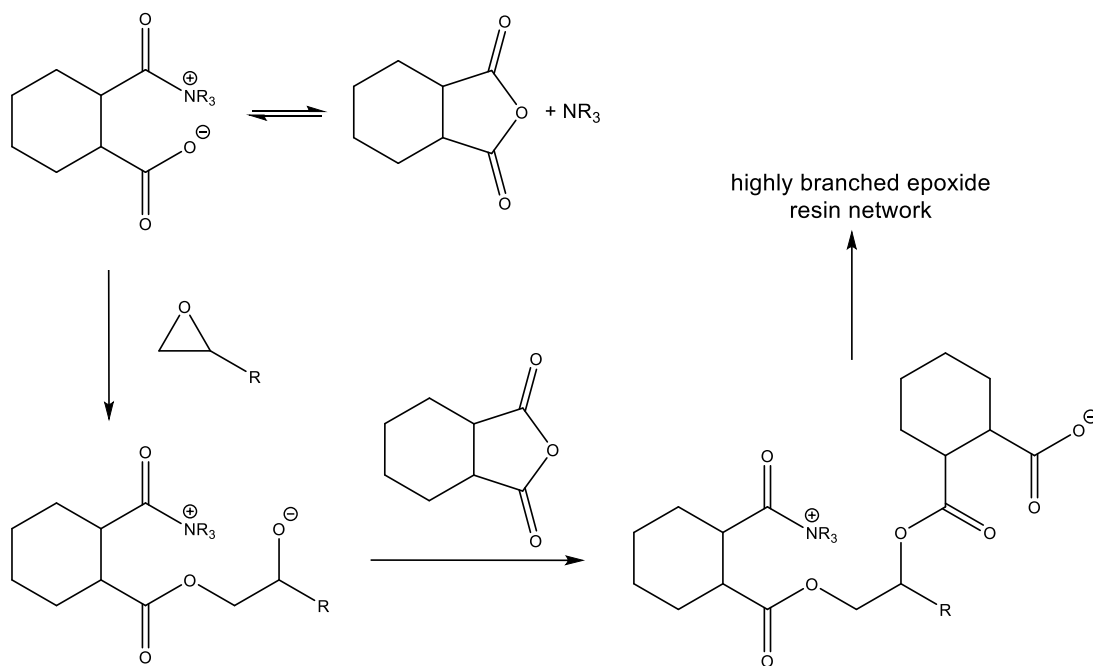
Scheme 12: Quaternary ammonium salt catalysed reaction mechanism for the polymerization of epoxy units with cyclic anhydrides.

For the preparation of the pristine and composite epoxy resin samples, the resin, the hardener and the corresponding amount of BN nanoparticles were mixed and mechanically stirred (i) at 400 rpm for the first 10 min and (ii) with a reduced speed

47

of 200 rpm for 3 h afterwards. After sonication at 60 °C for 3 h, the homogeneous emulsion was poured into a stainless steel sample holder with a sample diameter of 50 mm and a height of 5 mm. The samples were kept at 100 °C for 5 h and postcured at 140 °C for 8 h. In the case of pristine epoxide resin samples, the resulting specimen were perfectly transparent without any gas inclusions, whereas the sample preparation of 10 and 25 wt.-% BN nanocomposites caused immense problems concerning gas evolution during the curing process. Significantly better results were obtained when the oven was evacuated during the tempering process, although the pore size of the best samples received *via* that strategy was still up to 0.4 mm in diameter. Pouring flatter samples on a stainless steel plate covered with another plate of 2 mm height with a rectangular cutout resulted in specimen free of gas bubbles. Out of this plate, round samples were cut and polished for later heat conductivity measurements.

3.8 Thermal conductivity measurements

For the determination of the thermal conductivity of the samples, a guarded heat flow meter from TA Instruments of the type DTC 300 was used. The samples were cut from a rectangular specimen plate, grinded and polished yielding round samples with a diameter of 50 mm and heights between 2 and 4 mm. The samples were free of gas bubbles, and the filler was dispersed homogeneously all over the specimens. The addition of boron nitride nanopowder leads to a significant increase in the thermal conductivity of epoxide resins of the type Araldite CY225/Aradur HY925 (Table 7; Figure 33).

Table 7: Measured thermal conductivity values for epoxide resins with different weight load of BN nanofiller.

Temperature [K]	pristine epoxide resin #1	pristine epoxide resin #2	mean value pristine epoxide resin
303	0.183	0.179	0.1810
333	0.188	0.182	0.1850
363	0.197	0.200	0.1985
393	0.199	0.199	0.1990
423	0.199	0.199	0.1990
Temperature [K]	**10 wt.-% BN composite #1**	**10 wt.-% BN composite #2**	**mean value 10 wt.-% BN composite**
303	0.205	0.216	0.2105
333	0.212	0.221	0.2165
363	0.238	0.234	0.2360
393	0.232	0.229	0.2305
423	0.237	0.233	0.2350
Temperature [K]	**25 wt.-% BN composite #1**	**25 wt.-% BN composite #2**	**mean value 25 wt.-% BN composite**
303	0.247	0.270	0.2585
333	0.254	0.249	0.2515
363	0.276	0.246	0.2610
393	0.275	0.270	0.2725
423	0.274	0.271	0.2725

It has to be mentioned that the reproducibility of the results decreases with an increased filler loading, possibly resulting from the bad wetting of BN. This fact is clearly visible in the great range of variation in particular in the two 25 wt.-% curves (Scheme 33). The results were converted to percent values in reference to the starting values, revealing a possible improvement of a factor ~1.2 for 10 wt.-% loading with BN and a factor ~1.4 for 25 wt.-% BN loading.
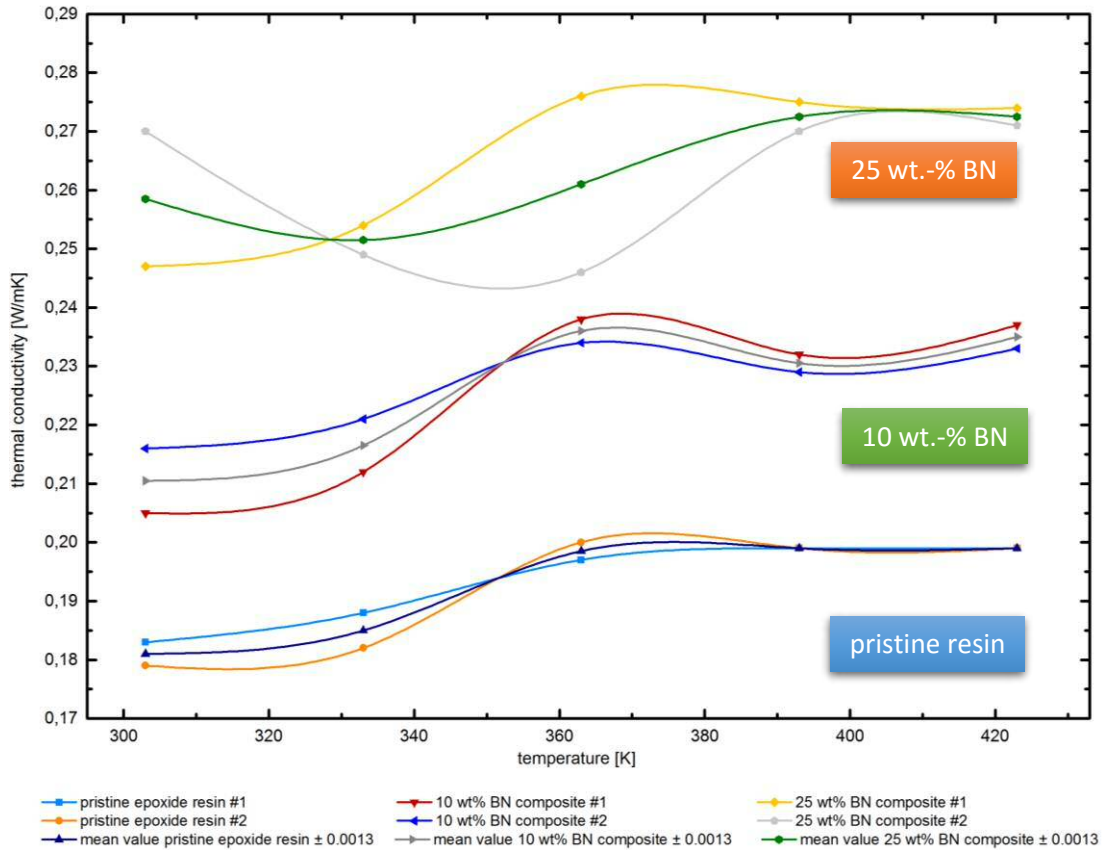
Figure 33: Heat transfer values of pristine epoxide resin compared with 10 and 25 wt.-% BN nanocomposites.

3.9 Permittivity measurements

In order to determine the electrical permittivity, square specimens with a size of 12x12 mm were cut from filled and unfilled epoxide resin samples and coated with conductive silver (Leitsilber 200, Ögussa). The measurements were performed on a Hewlett-Packard 4192A LF Impedance Analyzer 5 Hz – 13 MHz at a voltage of 1 V at different frequencies. For evaluation, the capacities equation (2-2) was used to

calculate the specific permittivity (Table 7). All permittivities were in the narrow range from 3.6-4.0.

$$C = \varepsilon_0 \cdot \varepsilon_r \cdot \frac{A}{l} \qquad \text{2-1}$$

$$\varepsilon_r = \frac{C \cdot l}{\varepsilon_0 \cdot A} \qquad \text{(2-2)}$$

C…capacity of an ideal capacitor F

ε_0…permittivity of vacuum $8.854 \cdot 10^{-12}$ $\dfrac{F}{m}$

ε_r…relative permittivity dimensionless
A…area of the capacitor m^2
l…distance between the capacitor between the plates [m]

Table 7: Values of the samples used for the determination of permittivity.

	pristine resin #1		10 wt.-% BN		25 wt.-% BN #1	
l [mm]	12.07		12.05		12.03	
b [mm]	11.92		11.95		11.88	
h [mm]	4.31		4.17		4.77	
A [mm²]	143.87		144.00		142.92	
l [m]	0.01207		0.01205		0.01203	
b[m]	0.01192		0.01195		0.01188	
h[m]	0.00431		0.00417		0.00477	
A[m²]	0.00014387		0.000144		0.00014292	
frequency [Hz]	capacity [pF]	loss factor	capacity [pF]	loss factor	capacity [pF]	loss factor
50	1.080	0.0950	1.211	0.0118	1.001	/
1.000	1.072	0.0105	1.201	0.0117	1.006	/
10.000	1.068	0.0113	1.205	0.0113	1.013	/
100.000	1.066	0.0117	1.223	0.0113	1.021	/
frequency [Hz]	permittivity		permittivity		permittivity	
50	3.65		3.96		3.77	
1.000	3.63		3.93		3.77	
10.000	3.61		3.94		3.81	
100.000	3.61		4.00		3.85	

3.10 Water uptake study

In order to determine the water uptake of the resin and the nanocomposites, which were previously used for heat conductivity measurements, the samples were weighed and placed into a humidity chamber at 30 °C and 85% relative humidity. Tests were performed in duplicate. In interval ranges of as close as 1 h, the samples were weighed on an analytical balance. The changes within the first hours of the experiment (Figure 34) are in the 0.1 per mil regime; trends in the different humidity uptake of the different samples are clearly visible. A direct correlation between weight load and humidity uptake cannot be drawn, since the 10 wt.-% samples show the highest water uptake, being followed by the 25 wt.-% samples; the resin itself shows the lowest water uptake. The wetting of the sample can still be directly connected to the nanofiller material, since the weight gain is higher in all four loaded samples than for the unloaded ones. The higher uptake of the 10 wt.-% sample can possibly be contributed to agglomeration of boron nitride with higher weight loads leading to smaller BN surface areas and therefore less exposure to humidity.
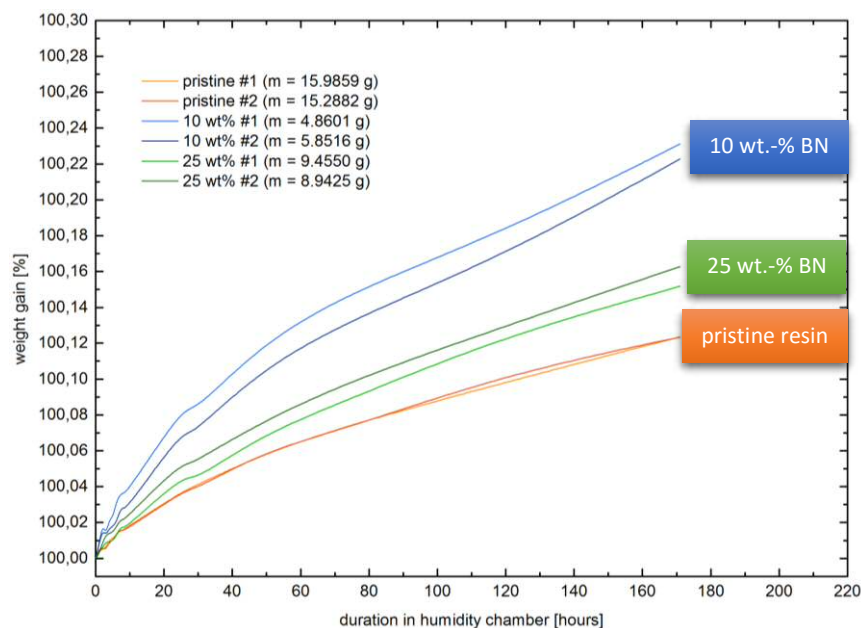
Figure 34: Water uptake of epoxide resin samples in reference to the residue time in the humidity chamber.

4. Conclusions & Outlook

Motivation and state-of-the-art. Since epoxide resins are widely used in high-voltage applications for both, packaging and isolation, their electronic and thermal performance is of high interest. Hence, the aim of this work was to improve the heat conductivity of a commercially available epoxy / anhydride resin, namely Araldite CY225 / Aradur HY925, without altering its electronic performance. Since boron nitride is a group III-V analogue to graphite, it possesses comparable thermal properties, but, due to the great ionic character of the covalent B-N bond, no electrical conductivity. This fact makes it a perfect candidate for the use as nanofiller in epoxide nanocomposites. The preparation of composites from polymer resins and boron nitride nanoparticles is challenging due to the insufficient wetting capabilities and the great hydrophobic character of the inorganic compound. Tailoring of these properties requires harsh reaction conditions due to the pronounced inertness of boron nitride.

Synthesis of borazine. One goal of this work was to mimic the whole synthetic process from single molecular precursors to the targeted product, namely boron nitride. The strategy published by Sneddon *et al.* in 1995 seemed to be a good strategy for the synthesis of BN. This polymer-ceramic route uses borazine as single-molecular precursor that readily dehydrogenizes to corresponding polyborazines, which can easily be pyrolyzed under inert conditions. Borazine is air- and moisture sensitive and, hence, has to be handled under inert conditions using Schlenk techniques. The reactants used for synthesis are $(NH_4)_2SO_4$ and $NaBH_4$, which are reacted in tetraethylene glycol dimethyl ether $[CH_3(OCH_2CH_2)_4OCH_3,$ tetraglyme]. All chemicals are easy and safe to handle at ambient conditions, making the synthesis the strategy of choice.

Despite the description as straight-forward approach to boron nitride, the synthesis of borazine according to the strategy by Sneddon *et al.* (Figure 35) turned out to be unexpectedly challenging, in particular due to unfavourably heavy foaming and product yields far below published values. Different modifications concerning chemicals (degassing and drying of the solvent, grinding and drying of $(NH_4)_2SO_4$) and apparatus (open inert system for the first hour of reaction, stepwise temperature increase) finally paved the way to the successful synthesis of borazine.
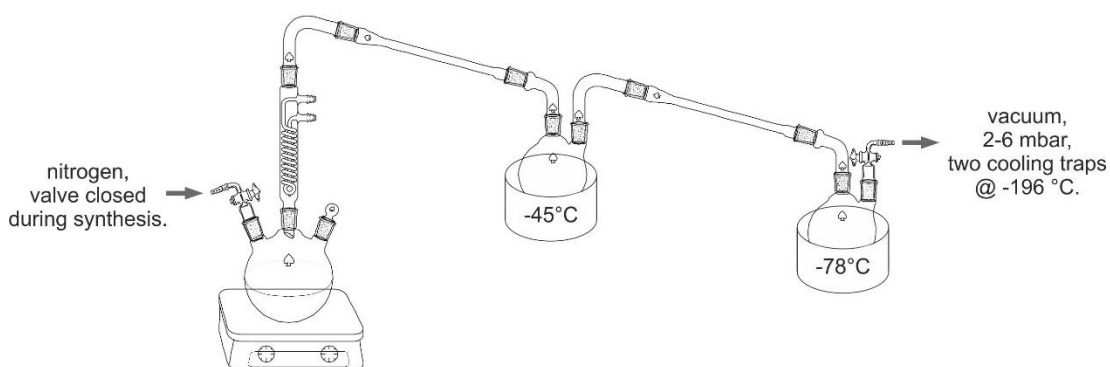
Figure 35: Apparatus used for the synthesis of borazine.

Synthesis of hexagonal boron nitride. In order to verify the general possibility of the synthesis of boron nitride from borazine and polyborazines, respectively, the synthetic route was investigated in detail. Preceded by the polymerization of borazine, boron nitride was obtained as brittle bulk material. ATR-IR investigations revealed slight impurities in the product, rendering the synthesis of boron nitride via the polymer route less recommendable for commercial use. Commercially available boron nitride nanopowder was fully characterized using SEM/EDX, XPS, DLS and ATR/IR spectroscopic techniques. These investigations revealed an average particle size of approx. 140 nm.

Preparation of boron nitride / epoxy nanocomposites. Using nanoscaled boron nitride as filler for the Araldite CY225 / Aradur HY925 epoxide resin, specimens with 0, 10, and 25 wt.-% of inorganic filler were produced. These samples were investigated in different ways, exploring (i) their possible improvement with respect to thermal conductivity, (ii) the influences of boron nitride on the electrical permittivity of epoxide resins, and (iii) the changes in their water uptake behavior.

Thermal conductivity and permittivity of boron nitride / epoxy nanocomposites. It could be shown that the thermal conductivity was increased by up to 40% for a 25 wt.-% filler loading compared to the pristine epoxide-anhydride resin. A load of 10 wt.-% BN was found to increase the thermal conductivity by up to 20%. Those modifications did not alter the electrical permittivity to significant extent: All permittivity values were between 3.6 and 4.0. Notably, a linear correlation between the filler content and permittivity could not be drawn.
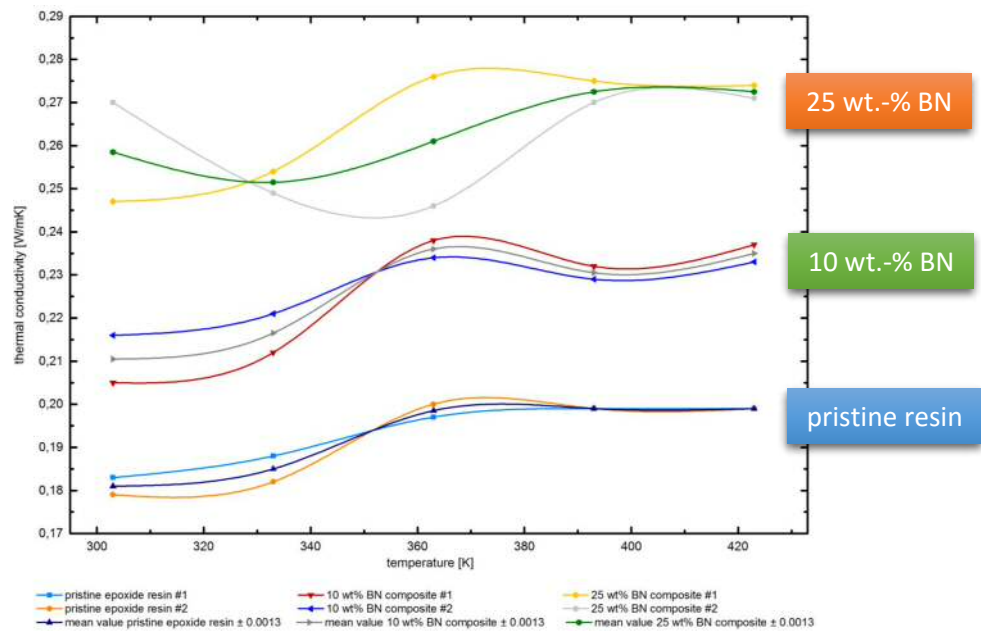
Figure 36: Heat transfer values of pristine epoxide resin compared with 10 wt.-% and 25 wt.-% BN nanocomposites

Water uptake of boron nitride / epoxy nanocomposites. The same conclusions could be drawn concerning the water uptake of the samples. It was shown that the presence of boron nitride within the samples enabled a higher water uptake than in the pristine epoxide resin; yet though again, no linear correlation could be found. This fact can be explained by agglomeration processes within the samples with higher weight loads, decreasing the exploited boron nitride surface to surrounding humidity and therefore limiting the water uptake.

Functionalization of boron nitride nanoparticles. For dedicated functionalization of the surfaces of the nanoparticles, reaction conditions for the surface oxidation (aiming to generate OH-functionalities) were evaluated in this study. The treatment of boron nitride with nitration acid (H_2SO_4 and HNO_3 in a ratio of 1:3) did not alter the chemical composition of the nanoparticles. Alternatively, the treatment of boron nitride nanopowder with piranha solution (H_2SO_4 and H_2O_2 in a ratio of 2:1) showed significant changes in the ATR-IR spectrum, revealing a broad OH vibrational signal. XPS investigations revealed a 4.0 % oxygen functionalization of boron nitride.

Outlook. High loadings of the epoxide resin with boron nitride nanoparticles (25 wt.-%) have increased the thermal conductivity of the corresponding composite to favourable 0.3 $Wm^{-1}K^{-1}$. Concomitant with such high filler loadings, agglomeration of the particles seems to occur. Hence, for optimum and highly reproducible production of such composites, boron nitride nanoparticles with functionalized nanoparticles should be used. The treatment of the particles with piranha solution, which was developed in this study, yields particles that can be correspondingly functionalized.

5. Experimental Section

5.1 Materials

Boron nitride nanoparticles were purchased from MKnano (Mississauga, Canada); the epoxy-anhydride resin was acquired from Huntsman (Basel, Switzerland). Deuterated solvents were supplied by euriso-top, Saint-Aubin Cedex, France. All other chemicals were purchased from Sigma Aldrich (Vienna, Austria). Purification methods have been detailed in the respective synthetic strategies.

5.2 Equipment

Infrared spectroscopy: All infrared spectra were recorded using a Bruker Alpha FT-IR spectrometer in ATR mode. The received spectra were processed using Opus 7.5 and Spekwin32. Prior to the measurements the background noise was recorded and afterwards subtracted.

NMR spectroscopy: ^{1}H- and ^{13}C-NMR spectra were recorded on a Bruker Ultrashield 300 MHz NMR machine coupled with a Bruker B-ACS 60 auto sampler that was controlled with Icon Automation NMR Software. Recorded spectra were processed using Topspin 3.1 and MestReNova 6.0.2-5475. ^{11}B-NMR spectra were recorded on a Varian Oxford NMR AS 500 spectrometer.

Dynamic Light Scattering measurements: The machine consist of a Coherent Verdi V5 green diode laser with a wavelength of 532 nm that is detected from a goniometer with single-mode fibre detection optics (OZ from GMP, Zürich, Switzerland) in a 90 ° angle. The signal is collected from an ALV/SO-SIPD/DUAL photomultiplier with pseudo-cross correlation and an ALV 7004 Digital Multiple Tau Real Time Correlator (ALV, Langen, Germany). The measurements consisted of 5

runs of each 30 seconds that were averaged by the ALV software package. The hydrodynamic radius was calculated using the optimized regulation technique software.[69]

DTA measurements: For the pyrolysis, a Netzsch STA 409 C/CD TG/DTA machine was used that was heated to 1400 °C with a heating rate of 5 K/min and a holding time of 3 h at the maximum temperature.

SEM/EDX measurements: SEM images were recorded on a Zeiss Ultra 55 scanning electron microscope that was operated at 20 kV. The specimens were sputtered with gold for 90 seconds prior investigation.

Light microscope: Light microscopic pictures were recorded using an Olympus BX 60 microscope in incident-light mode.

Thermal conductivity measurements: For the determination of the heat transfer values, a DTC 300 guarded heat flow meter from TA Instruments (New Castle, USA) was used. Received data were processed using Model 2022 Data Analysis Software 5.0 from Anter Corporation.

Permittivity measurements: Permittivity values were determined using a Hewlett-Packard 4192A LF Impedance Analyzer 5 Hz-13 MHz with a Hewlett Packard 16334A Test Fixture mounted. The specimens were coated with conductive silver (Leitsilber 200, Ögussa) prior to measurements.

X-ray photoelectron spectroscopy: XPS spectra were recorded on a Thermo Scientific K-Alpha+ X-ray Photoelectron Spectrometer (XPS) System and processed with the Thermo Scientific Avantage Software for surface analysis.

Karl-Fisher titration: In order to determine the water content of solvents, a Mitsubishi CA-100 Coulometric Moisture Meter was used.

5.3 Synthetic procedures

The synthesis of borazine and polyborazine was performed using standard Schlenk techniques with pre-dried nitrogen as inert gas.

5.3.1 Synthesis of borazine according to Bernhard et al.

$$NaBH_4 + (NH_4)_2SO_4 \xrightarrow[\substack{8h}]{\substack{tetraglyme \\ 120°C}}$$
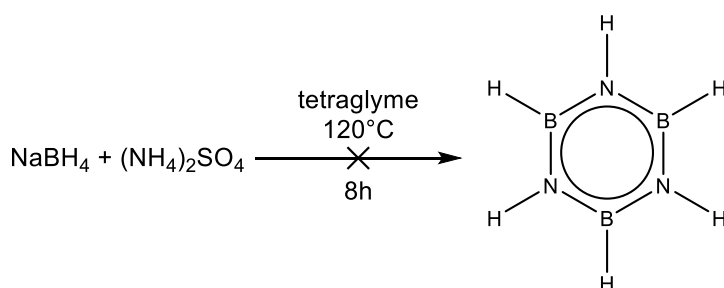
Scheme 13: Synthesis of borazine according to Bernard and Sneddon.[23,30]

Table 8: Quantities of used chemicals for the synthesis of borazine.

	M [g mol^{-1}]	m [g]	n [mmol]	V [mL]	eq.
(NH$_4$)$_2$SO$_4$	132.14	46.49	351.8	-	1.3
NaBH$_4$	37.83	10.26	271.2	-	1
tetraglyme	222.28	-	-	100	solvent

As described by Bernard et al. in 2009,[23] all chemicals were used as purchased. 46.49 g (NH$_4$)$_2$SO$_4$ (351.8 mmol, 1.3 eq.) were weighed in, heated with a heat gun and dried on a high dynamic vacuum for 1 h. After nitrogen inert gas was flushed through the apparatus, 10.26 g NaBH$_4$ (271.2 mmol, 1 eq.) were added, and the solids were mixed using a magnetic stirrer. 100 mL of tetraglyme were added. Even at room temperature, heavy foaming occurred. When foaming decreased, the

reaction vessel was slowly heated to 120 °C, what restarted heavy foaming. No vacuum could be applied, rendering the isolation of borazine impossible.

5.3.2 Synthesis of borazine according to Li et al.

$$NaBH_4 + (NH_4)_2SO_4 \xrightarrow[\substack{AlCl_3}]{\substack{tetraglyme \\ 45\ °C \\ 8\ h}}$$
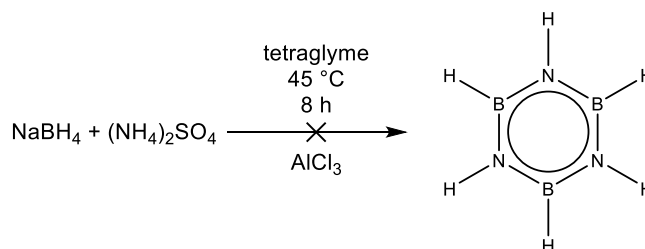
Scheme 14: Synthesis of borazine according to Li.[33]

Table 9: Quantities of used chemicals for the synthesis of borazine.

	M [g mol⁻¹]	m [g]	n [mmol]	V [mL]	eq.
(NH₄)₂SO₄	132.14	25.08	189.8	-	1
NaBH₄	37.83	10.02	264.9	-	1.4
AlCl₃	133.34	0.3502	2.63	-	0.01
tetraglyme	222.28	-	-	100	solvent

Described by Li *et al.* in 2011,[33] only small modifications were applied to the reactants. $(NH_4)_2SO_4$ was finely ground and dried in an oven at 120 °C for 3 days. 25.08 g $(NH_4)_2SO_4$ (189.8 mmol, 1 eq.) were heated with a heat gun and dried on a high dynamic vacuum for 1 h. After nitrogen inert gas was flushed through the apparatus, 350 mg $AlCl_3$ (2.63 mmol, 0.01 eq.) were added. The apparatus was evacuated for 1 h and again flushed with nitrogen inert gas. 10.02 g $NaBH_4$ (264.9 mmol, 1.4 eq.) dissolved in 100 mL of tetraglyme were slowly added to the reactant mixture, during which foaming occurred. No products could be isolated in the cooling traps at −80 and −196 °C.

5.3.3 Synthesis of borazine according to Li et al. (Modification 1)
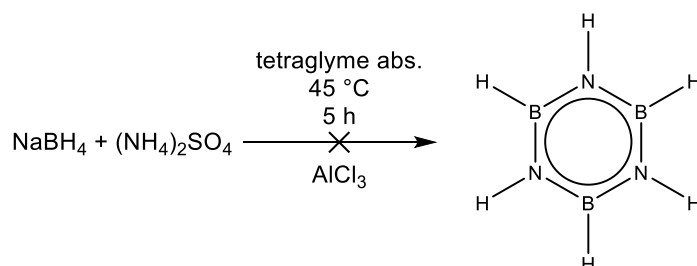
Scheme 15: Synthesis of borazine according to Li.[33]

Table 10: Quantities of used chemicals for the synthesis of borazine.

	M [g mol^{-1}]	m [g]	n [mmol]	V [mL]	eq.
(NH$_4$)$_2$SO$_4$	132.14	25.00	189.2	-	1
NaBH$_4$	37.83	10.04	265.4	-	1.4
AlCl$_3$	133.34	0.3594	2.70	-	0.01
tetraglyme abs	222.28	-	-	100	solvent

Tetraglyme was degassed on a high dynamic vacuum for 1 h and dried with the help of molecular sieves 3A. Karl-Fisher titration showed a final water content of 20 ppm in contrast to 100 ppm prior to drying. 25.00 g (NH$_4$)$_2$SO$_4$ (189.2 mmol, 1 eq.) were heated with a heat gun and dried on a high dynamic vacuum for 1 h. After nitrogen inert gas was flushed through the apparatus, 359 mg AlCl$_3$ (2.70 mmol, 0.01 eq.) were added. The apparatus was evacuated for 1 h and again flushed with nitrogen inert gas. 10.04 g NaBH$_4$ (265.4 mmol, 1.4 eq.) dissolved in 100 mL of dry tetraglyme were slowly added to the reactants. The mixture was stirred in inert atmosphere at 45 °C for 1 h. Subsequently, vacuum was applied and volatile collected in cooling traps of −80 and −196 °C. 0.1 mL of borazine as transparent liquid together with a white residue could be collected in the −80 °C trap.

5.3.4 Synthesis of borazine according to Li et al. (Modification 2)

Scheme 16: Synthesis of borazine according to Li.[33]

Table 11: Quantities of used chemicals for the synthesis of borazine.

	M [g mol^{-1}]	m [g]	n [mmol]	V [mL]	eq.
(NH$_4$)$_2$SO$_4$	132.14	25.05	189.6	-	1
NaBH$_4$	37.83	10.00	264.3	-	1.4
AlCl$_3$	133.34	0.3531	2.65	-	0.01
tetraglyme abs	222.28	-	-	100	solvent

25.05 g dry (NH$_4$)$_2$SO$_4$ (189.6 mmol, 1 eq.) were heated with a heat gun and dried on a high dynamic vacuum for 1 h. After nitrogen inert gas was flushed through the apparatus, 353 mg AlCl$_3$ (2.65 mmol, 0.01 eq.) and 10.00 g NaBH$_4$ (264.3 mmol, 1.4 eq.) were added. The apparatus was evacuated for 1 h and again flushed with nitrogen inert gas. 100 mL of dry tetraglyme were added and the reaction mixture was stirred at 45 °C for 24 h. Subsequently, all volatile parts were removed on a high dynamic vacuum and trapped at −196 °C. Only polyaminoborane (BH$_2$NH$_2$)$_n$ could be isolated as white solid. Repetition of the experiment at a temperature of 100 °C yielded a significant amount of polyaminoborane (BH$_2$NH$_2$)$_n$, but again no borazine.

5.3.5 Synthesis of borazine according to Wideman

Scheme 17: Synthesis of borazine according to Wideman.[65]

Table 12: Quantities of used chemicals for the synthesis of borazine.

	M [g mol^{-1}]	m [g]	n [mmol]	V [mL]	eq.
(NH$_4$)$_2$SO$_4$	132.14	26.80	202.8	-	1.3
NaBH$_4$	37.83	10.00	264.3	-	1
tetraglyme	222.28	-	-	50	solvent

26.80 g (NH$_4$)$_2$SO$_4$ (202.8 mmol, 1.3 eq.) were heated with a heat gun and dried on a high dynamic vacuum. After nitrogen inert gas was flushed through the apparatus, 10.00 g NaBH$_4$ (202.8 mmol, 1 eq.) were added, and the solids were mixed using a magnetic stirrer. The apparatus was evacuated and again flushed with nitrogen. 50 mL of dry tetraglyme were added, and the reaction mixture was stirred in inert atmosphere at 80 °C. After 1 h, vacuum was applied and volatile compounds collected in cooling traps of −45, −80, and −196 °C, while the temperature of the reaction vessel was increased to 140 °C. In the −80 °C trap, 2.63 g of borazine (with a 20% fraction of μ-aminodiborane) could be collected (26.13 mmol, 10% yield).

^{1}H NMR (CDCl$_3$): δ [ppm] = 4.34 (3 H, q, B*H*), 5.54 (3 H, t, N*H*).

^{11}B NMR (CDCl$_3$): δ [ppm] = 30.62 (d, N*B*HN, J = 140.92 Hz).

IR: ν [cm^{-1}] = 3455 (m), 2503 (m), 1438 (s), 1359 (m), 903 (s), 720 (m).

5.3.6 Synthesis of polyborazine according to Sneddon and Remsen
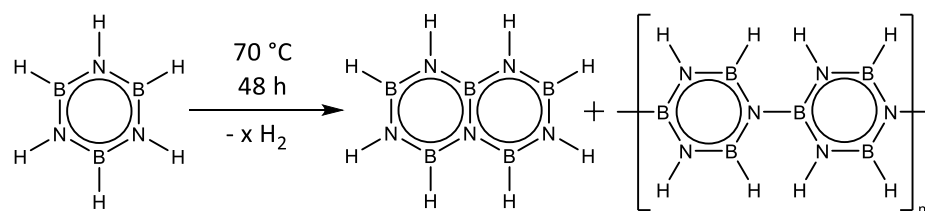
Scheme 18: Synthesis of polyborazine according to Sneddon and Remsen.[40]

Table 13: Quantities of used chemicals for the synthesis of polyborazine.

	M [g mol^{-1}]	m [g]	n [mmol]	V [mL]	eq.
borazine	80.53	0.498	6.18	0.6	1

0.6 mL of a borazine / μ-aminodiborane mixture (0.498 g) were heated under nitrogen inert gas at 70 °C for 48 h. Subsequently, all volatile parts were removed using a high dynamic vacuum. The resulting gel-like residue was dissolved in 5 mL of absolute tetraglyme in an argon-filled glove box. The polymer was precipitated in 50 mL of dry pentane, filtered off using a frit with a pore size of 4 at ambient conditions and dried on a high dynamic vacuum, yielding 0.495 g (99%) of a white powder-like solid.

^{11}B NMR (CDCl$_3$): δ [ppm] = 20.48 (br).

IR: ν [cm^{-1}] = 3253 (br), 2971 (m), 2392 (br), 1398 (m), 1261 (s), 1010 (s), 793 (s), 701 (m), 472 (m).

5.3.7 Synthesis of boron nitride
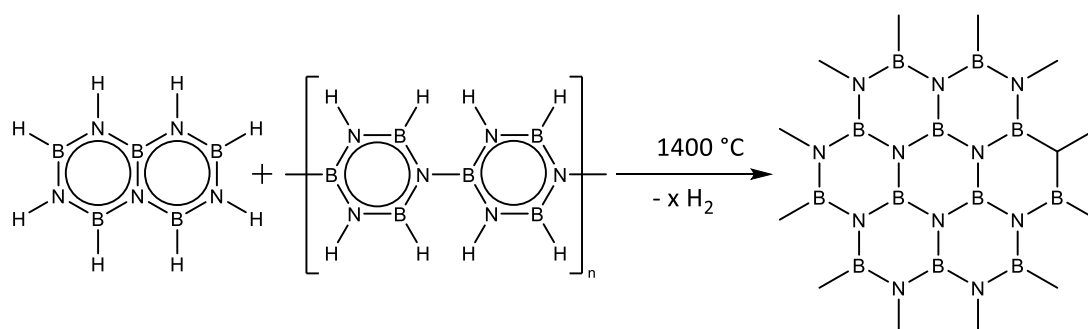
Scheme 19: Pyrolysis of PBZ to BN.

Table 14: Quantities of used chemicals for the synthesis of boron nitride.

	M [g mol⁻¹]	m [mg]	n [mmol]	V [mL]	eq.
polyborazine	-	122.118	-	-	-

122.118 mg polyborazine were weighed in an Al_2O_3 DTA crucible. The sample was heated to 1400 °C with a holding time of 3 h and a heating rate of 5 K/min in inert conditions (N_2, 40 mL/min). 120 mg of transparent residue were recovered (yield: 98.5 %).

IR: v [cm⁻¹] = 1219 (s), 997 (w), 840 (w), 760 (m), 725 (m), 612 (s).

5.4 Epoxide resin sample preparation

In a standard procedure, 100 g of CY225 resin were mechanically mixed with 80 g of HY925 hardener using a KPG-stirrer with movable stainless steel blades. Initially, the speed was set to 400 rpm for 10 min and subsequently reduced to 200 rpm for 2.5 h. The corresponding amount of BN nanopowder was added, and the solution was degassed at 60 °C using an ultrasonic bath. After the solution was free of any

gas cavities, it was poured into a stainless steel form with a size of 16 x 11 cm and a height of 2 mm that was cleaned with Chemlease Mold Cleaner EZ and Chemlease R&B EZ. The samples were kept in a vacuum drying oven at 300 mbar and 60 °C for 30 min, heated to 100 °C for 5 h and post-cured at 140 °C for 8 h. The resulting specimens were transparent and of yellow color (pristine resin) or white and opaque (10 and 25 wt.-% BN) with a perfectly smooth surface.

5.5 Boron nitride characterization

SEM/EDX sample preparation: 7.5 mg boron nitride (modified and unmodified) were dispersed in 15 g of EtOH abs., yielding a 0.05 wt.-% solution. 1 mL of this solution was diluted with 4 mL of EtOH abs., yielding a 0.01 wt.-% solution. These solutions were spincast on silicon wafers (5 seconds, 4000 rpm, 2500 rpm/s) and dried in an oven at 60 °C.

Dynamic light scattering sample preparation: 7.5 mg boron nitride (modified and unmodified) were dispersed in 15 g of EtOH abs., yielding a 0.05 wt.-% solution. 1 mL of this solution was diluted with 4 ml of EtOH abs., yielding a 0.01 wt.-% solution.

5.6 Boron nitride activation

250 mg boron nitride were dispersed in nitration acid that was freshly prepared from 15 mL concentrated nitric acid and 5 mL concentrated sulfuric acid at 0 °C. The emulsion was sonicated at 60 °C for 6 h and kept at vigorous stirring at 80 °C for 72 h afterwards. After 72 h, the reaction mixture was transferred into a PP vessel and centrifuged at 4500 rpm for 10 min. The supernatant was rejected, the residue washed with deionized water and the emulsion centrifuged again with the same parameters. The procedure was repeated until the supernatant was pH neutral. The

white solid residue was dissolved in acetone, transferred into a crystallizing dish and dried in an oven at 80 °C for 72 h, yielding 206 mg (82%) of a white powder.

IR: v [cm^{-1}] = 3200 (br), 1346 (s), 1200 (s), 1050(m), 890 (w), 760 (s), 590 (w).

5.7 Sample preparation for impedance measurements

From the epoxide resin samples that were prepared as described above, square specimens were cut and coated with conductive silver (Leitsilber 200, Ögussa). The coating was dried at 80 °C for 10 min on each side.

5.8 Water uptake study

In order to determine the water uptake of the samples that were earlier used for heat conductivity measurements, the samples were weighed and stored in a humidity chamber at 30 °C and 85% relative humidity. In an interval of 1 h, the samples were taken out of the chamber and weighed using an analytic balance.

6. Bibliography

1.   Moore, G. E. Cramming more components onto integrated circuits (Reprinted from Electronics, pg 114-117, April 19, 1965). *Proc. Ieee* **86,** 82–85 (1998).

2.   Clark, D. Intel rechisels the Tablet on Moore's law. *Wall Street Journal Digits Tech News and Analysis* (2015).

3.   Xie, B. H., Huang, X. & Zhang, G. J. High thermal conductive polyvinyl alcohol composites with hexagonal boron nitride microplatelets as fillers. *Compos. Sci. Technol.* **85,** 98–103 (2013).

4.   Chen, Y.-M. & Ting, J.-M. Ultra high thermal conductivity polymer composites. *Carbon N. Y.* **40,** 359–362 (2002).

5.   Wong, C. P. & Bollampally, R. S. Thermal conductivity, elastic modulus, and coefficient of thermal expansion of polymer composites filled with ceramic particles for electronic packaging. *J. Appl. Polym. Sci.* **74,** 3396–3403 (1999).

6.   Cho, H. B. *et al.* Self-assemblies of linearly aligned diamond fillers in polysiloxane/diamond composite films with enhanced thermal conductivity. *Compos. Sci. Technol.* **72,** 112–118 (2011).

7.   Powell, R. W., Ho, C. Y. & Liley, P. E. *CRC Handbook of Chemistry and Physics*. (The Chemical Rubber Company, 1970).

8.   Brandrup, J., Immergut, E. & Grulke, E. A. *Polymer Handbook*. *John Wiley & Sons, Inc* **12,** (John Wiley & Sons, Inc., 1990).

9.   Royal, T. H. E., Academy, S. & Sciences, O. F. *Graphene*. *Scientific Background on the Nobel Prize in Physics 2010* (2010). doi:10.1038/news.2010.620

10. Czichos (Hrsg.), H. in *Die Grundlagen der Ingenieurwissenschaften* 54 (Springer, 2000).

11. Leichtfried, G. in *Group VIII Advanced Materials and Technologies: Powder Metallurgy Data. Refractory, Hard and Intermetallic Materials* 118–139 (Springer, 2002).

12. Hou, J. *et al.* Preparation and Characterization of Surface Modified Boron Nitride Epoxy Composites with Enhanced Thermal Conductivity. *RSC Adv.* **4,** 44282–44290 (2014).

13. Huang, X., Zhi, C. & Jiang, P. Toward effective synergetic effects from graphene nanoplatelets and carbon nanotubes on thermal conductivity of ultrahigh volume fraction nanocarbon epoxy composites. *J. Phys. Chem. C.* **116,** 23812–23820 (2012).

14. Fang, L. *et al.* Nano–micro structure of functionalized boron nitride and aluminum oxide for epoxy composites with enhanced thermal conductivity and breakdown strength. *RSC Adv.* **4,** 21010 (2014).

15. Andritsch, T. Epoxy Based Nanodielectrics for High Voltage DC Applications: Synthesis, Dielectric Properties and Space Charge Dynamics. (Technische Universiteit Delft, 2010).

16. Liem, H. & Choy, H. S. Superior thermal conductivity of polymer nanocomposites by using graphene and boron nitride as fillers. *Solid State Commun.* **163,** 41–45 (2013).

17. Sōma, T., Sawaoka, A. & Saito, S. Characterization of wurtzite type boron nitride synthesized by shock compression. *Mater. Res. Bull.* **9,** 755–762 (1974).

18. Bernard, S. & Miele, P. Polymer-derived boron nitride: A review on the chemistry, shaping and ceramic conversion of borazine derivatives. *Materials (Basel).* **7,** 7436–7459 (2014).

19. Weng, Q., Wang, X., Wang, X., Bando, Y. & Golberg, D. Functionalized hexagonal boron nitride nanomaterials: emerging properties and applications. *Chem. Soc. Rev.* (2016). doi:10.1039/C5CS00869G

20. Lin, Y. *et al.* Aqueous dispersions of few-layered and monolayered hexagonal boron nitride nanosheets from sonication-assisted hydrolysis: Critical role of water. *J. Phys. Chem. C* **115,** 2679–2685 (2011).

21. Eichler, J. & Lesniak, C. Boron nitride (BN) and BN composites for high-temperature applications. *J. Eur. Ceram. Soc.* **28,** 1105–1109 (2008).

22. Pease, R. S. An x-ray study of boron nitride. *Acta Crystallogr.* **5,** 356–361 (1952).

23. Salles, V. *et al.* Design of highly dense boron nitride by the combination of spray-pyrolysis of borazine and additive-free sintering of derived ultrafine powders. *Chem. Mater.* **21,** 2920–2929 (2009).

24. Paine, R. T., Narula, C. K., Schaeffer, R. & Datye, A. Synthesis of Boron Nitride Ceramics from 2,4,6-Triaminoborazine. *Inorg. Chem.* **28,** 4053–4055 (1989).

25. Lipp, A., Schwetz, K. A. & Hunold, K. Hexagonal boron nitride: Fabrication, properties and applications. *J. Eur. Ceram. Soc.* **5,** 3–9 (1989).

26. Chantrell, P. G. & Popper, E. P. *Inorganic Polymers and Ceramics. Special Ceramics* **4,** (Academic Press, 1964).

27. Bernard, S., Salameh, C. & Miele, P. Boron nitride ceramics from molecular precursors: synthesis, properties and applications. *Dalt. Trans.* 861–873 (2016). doi:10.1039/C5DT03633J

28. Colombo, P., Mera, G., Riedel, R. & Sorarù, G. D. Polymer-Derived Ceramics: 40 Years of Research and Innovation in Advanced Ceramics. *J. Am. Ceram. Soc.* **93,** no–no (2010).

29. Pohland, E. & Stock, A. Borwasserstoffe, IX: B3N3H6. *Ber. Dtsch Chem. Ges.* **59,** 2215–2223 (1926).

30. Wideman, T., Sneddon, L. G., T.Widman & L.G.Sheddon. Convenient Procedures for the Laboratory Preparation of Borazine. *Inorg. Chem.* **34,** 1002–1003 (1995).

31. Bechelany, M. *et al.* Synthesis of boron nitride nanotubes by a template-assisted polymer thermolysis process. *J. Phys. Chem. C* **111,** 13378–13384 (2007).

32. Duperrier, S. *et al.* Design of a series of preceramic B-tri(methylamino)borazine-based polymers as fiber precursors: Architecture, thermal behavior, and melt-spinnability. *Macromolecules* **40,** 1018–1027 (2007).

33. Li, J. S., Zhang, C. R., Li, B., Cao, F. & Wang, S. Q. An improved synthesis of borazine with aluminum chloride as catalyst. *Eur. J. Inorg. Chem.* **5,** 1763–1766 (2010).

34. Schellenberg, R., Kriehme, J. & Wolf, G. Thermal decomposition of cyclotriborazane. *Thermochim. Acta* **457,** 103–108 (2007).

35. Wang, J. S. & Geanangel, R. A. 11B NMR studies of the thermal decomposition of ammoniaborane in solution. *Inorganica Chim. Acta* **148,** 185–190 (1988).

36. Gaines, D. Studies of boron-Nitrogen Compounds. VIII. 1 Nuclear Magnetic Resonance Studies of Some μ-Aminodiboranes and Amine Boranes. *J. Am. Chem.* **552,** 1961–1963 (1964).

37. Li, J., Zhang, C., Li, B., Cao, F. & Wang, S. An investigation on the synthesis of borazine. *Inorganica Chim. Acta* **366,** 173–176 (2011).

38. Chen, X., Zhao, J. C. & Shore, S. G. Facile synthesis of aminodiborane and inorganic butane analogue NH 3BH2NH2BH3. *J. Am. Chem. Soc.* **132,** 10658–10659 (2010).

39. Li, H. *et al.* Formation Mechanisms, Structure, Solution Behavior, and Reactivity of Aminodiborane. *J. Am. Chem. Soc.* **137,** 12406–12414 (2015).

40. Fazen, P. J. *et al.* Synthesis, Properties, and Ceramic Conversion Reactions of Polyborazine. A High-Yield Polymeric Precursor to Boron Nitride. *Chem. Mater.* **7,** 1942–1956 (1995).

41. Li, J., Bernard, S., Salles, V., Gervais, C. & Miele, P. Preparation of Polyborazine-Derived Bulk Boron Nitride with Tunable Properties by Warm-Pressing and Pressureless Pyrolysis. *Chem. Mater.* **22,** 2010–2019 (2010).

42. Becker, R. *et al. Gmelin Handbuch der Anorganischen Chemie*. (Springer-Verlag, 1978).

43. Huang, X. *et al.* Thermally conductive, electrically insulating and melt-processable polystyrene/boron nitride nanocomposites prepared by *in situ*

reversible addition fragmentation chain transfer polymerization. *Nanotechnology* **26,** 015705 (2015).

44. Zhi, C. Y. *et al.* Chemically activated boron nitride nanotubes. *Chem. - An Asian J.* **4,** 1536–1540 (2009).

45. Zhi, C. *et al.* Towards thermoconductive, electrically insulating polymeric composites with boron nitride nanotubes as fillers. *Adv. Funct. Mater.* **19,** 1857–1862 (2009).

46. Coleman, J. N. *et al.* Two-Dimensional Nanosheets Produced by Liquid Exfoliation of Layered Materials. *Science (80-.).* **331,** 568–571 (2011).

47. Wang, X. *et al.* 'Chemical blowing' of thin-walled bubbles: High-throughput fabrication of large-area, few-layered BN and C x-BN nanosheets. *Adv. Mater.* **23,** 4072–4076 (2011).

48. Sainsbury, T. *et al.* Oxygen radical functionalization of boron nitride nanosheets. *J. Am. Chem. Soc.* **134,** 18758–18771 (2012).

49. Lee, D. *et al.* Scalable exfoliation process for highly soluble boron nitride nanoplatelets by hydroxide-assisted ball milling. *Nano Lett.* **15,** 1238–1244 (2015).

50. Xiao, F. *et al.* Edge-Hydroxylated Boron Nitride Nanosheets as an Effective Additive to Improve the Thermal Response of Hydrogels. *Adv. Mater.* **27,** 7196–7203 (2015).

51. Huang, X. *et al.* Polyhedral oligosilsesquioxane-modified boron nitride nanotube based epoxy nanocomposites: An ideal dielectric material with high thermal conductivity. *Adv. Funct. Mater.* **23,** 1824–1831 (2013).

52. Wang, X. Bin *et al.* Biomass-directed synthesis of 20 g high-quality boron nitride nanosheets for thermoconductive polymeric composites. *ACS Nano* **8,** 9081–9088 (2014).

53. Zhu, H. *et al.* Highly thermally conductive papers with percolative layered boron nitride nanosheets. *ACS Nano* **8,** 3606–3613 (2014).

54. Song, W. L. *et al.* Polymer/boron nitride nanocomposite materials for superior thermal transport performance. *Angew. Chemie - Int. Ed.* **51,** 6498–6501 (2012).

55. Novoselov, K. S. *et al.* Electric Field Effect in Atomically Thin Carbon Films. *Science (80-.).* **306,** 666–669 (2004).

56. Novoselov, K. S. *et al.* Two-dimensional atomic crystals. *Proc. Natl. Acad. Sci. U. S. A.* **102,** 10451–10453 (2005).

57. Pakdel, A., Bando, Y. & Golberg, D. Nano boron nitride flatland. *Chem. Soc. Rev.* **43,** 934–59 (2014).

58. Charlier, J.-C., Blase, X., De Vita, A. & Car, R. Microscopic growth mechanisms for carbon and boron-nitride nanotubes. *Appl. Phys. A* **68,** 267–273 (1999).

59. Pakdel, A., Zhi, C., Bando, Y. & Golberg, D. Low-dimensional boron nitride nanomaterials. *Mater. Today* **15,** 256–265 (2012).

60. Li, L. H. *et al.* Large-scale mechanical peeling of boron nitride nanosheets by low-energy ball milling. *J. Mater. Chem.* **21,** 11862 (2011).

61. Zhi, C., Bando, Y., Tang, C., Kuwahara, H. & Golberg, D. Large-Scale Fabrication of Boron Nitride Nanosheets and Their Utilization in Polymeric

Composites with Improved Thermal and Mechanical Properties. *Adv. Mater.* **21,** 2889–2893 (2009).

62.   Li, X. *et al.* Exfoliation of hexagonal boron nitride by molten hydroxides. *Adv. Mater.* **25,** 2200–4 (2013).

63.   Yurdakul, H. *et al.* Nanoscopic characterization of two-dimensional (2D) boron nitride nanosheets (BNNSs) produced by microfluidization. *Ceram. Int.* **38,** 2187–2193 (2012).

64.   Chen, X., Dobson, J. F. & Raston, C. L. Vortex fluidic exfoliation of graphite and boron nitride. *Chem. Commun.* **48,** 3703 (2012).

65.   Wideman, T. *et al.* in *Inorganic Syntheses* 232–242 (John Wiley & Sons, Inc., 1998). doi:10.1002/9780470132630.ch39

66.   Armstrong, D. R. The electronic structure of aminodiborane. *Inorganica Chim. Acta* **18,** 145–146 (1976).

67.   Geick, R., Perry, C. H. & Rupprecht, G. Normal Modes in Hexagonal Boron Nitride. *Phys. Rev.* **146,** 543–547 (1966).

68.   Diaz-chacon, L. *et al.* Graphite Nanoplatelets Composite Materials : Role of the Epoxy-System in the Thermal Conductivity. *J. Mater. Sci. Chem. Eng.* **3,** 75–87 (2015).

69.   Schnablegger, H. & Glatter, O. Optical sizing of small colloidal particles: an optimized regularization technique. *Appl. Opt.* **30,** 4889–4896 (1991).

Curriculum Vitae

PERSONAL DATA

Name:	**Martin Rausch**, BSc.
Address:	Kasernstraße 21/b/9
	8053 Graz
	Austria
Telephone:	+43/0/664 7501 7469
Email:	mat.rausch@gmail.com
Nationality:	Austria
Date of Birth:	04.10.1990
Place of Birth:	Graz, Austria

EDUCATION

03/2014 – 09/2016   **Master Program Technical Chemistry**, Graz University of Technology and University of Graz

> *Main focus on Macromolecular Chemistry and Technology.*

03/2016 – 09/2016   **Master Thesis**, Graz University of Technology, Institute for Chemistry and Technology of Materials, Prof. Frank Wiesbrock

> *Enhancing the Thermal Conductivity of Epoxide Resins with Boron Nitride Nanofillers.*

10/2010 – 02/2014   **Bachelor Program Chemistry**, Graz University of Technology and University of Graz

Bachelor Thesis, Graz University of Technology, Institute of Inorganic Chemistry, Prof. Harald Stüger

> *Silicon-Carbon double bond systems – photo induced rearrangement of acylsilanes and the formation of unknown silenolates.*

09/2001 – 06/2009   **Bundesrealgymnasium Oeverseegasse**, Graz

Degree with distinction

Outgoings

06/2012 – 07/2012	**Research Work** at the Univerzitet u Novom Sadu in Novi Sad, Serbia, Prof. Janoš Canadi
	Regioselective Oxidation of Cholic Acid.

Work Experience

Since 11/2015	**Climbing Instructor,** BlocHouse Graz, City Adventure Center Graz
	Instruction of beginners and skilled climbers, break down of complex processes to small pieces that can easily be understood, handling of risky situations and procedures.
Since 10/2013	**Student Supervisor**, Graz University of Technology, Institute for Chemistry
	Supervision of students in the laboratory for inorganic chemistry.
	Teaching general chemistry class for process engineers.
Since 10/2012	**Project Worker**, Graz University of Technology, Institute of Inorganic Chemistry, Prof. Harald Stüger
	Inorganic and Organic Synthesis, full characterization of organometallic compounds.
11/2012 – 03/2013	**Photographer**, Ballguide Photoservice, Graz
11/2007 – 03/2012	**Photographer**, Foto Schmickl, Lassnitzhöhe
	Studio (portrait, family) and outdoor photo sessions (weddings, proms, baptisms, concerts).
10/2010 – 06/2011	**Prop Master**, Schauspielhaus Graz
	Stage design, organization of the backstage schedule, artists' liaison.
10/2009 – 06/2010	**Civilian Service,** Jugend am Werk Steiermark, Zentrum R6
	Youth Welfare – coordination in rehabilitation, mentorship and guidance of troubled teenagers.

Since 07/2005   **Windsurf Instructor**, various different schools, since 2014 for the Institute of Sports of the University of Graz, Graz and Neusiedler See

Lead group seminars, teach complex motion sequences, instruction and motivation of beginners and skilled students.

MEMBERSHIP

Since 07/2015   **Alpenverein**, Akademische Sektion Graz – volunteer work as team leader

Head of 40+ volunteers that give courses and trainings in different mountain sports areas. Coordination of responsibilities and processes within the team.

Since 10/2012   **Alpenverein,** Akademische Sektion Graz – volunteer work as youth leader

Trainer for alpine and sports climbing, mountaineering and freeriding; organizing trips and giving courses and trainings in different mountaineering areas. Contribution in sports camps for children. Contributions in different activities for people with migration background.

06/2010 – 06/2015   **Alumni of Oeverseegymnasium Graz**, Beirat

Supporting less fortunate children and school's community.

09/2007 – 07/2008   ***School Representative at Oeverseegymnasium Graz***

Organizing communication seminars and courses for project management for pupils, organizing a panel discussion before the Graz local election 2008, organizing a Graz-wide sports competition.

Languages	German (mother tongue), English (C1+), Spanish (A1), Latin.
IT- Knowledge	MS-Office, SciFinder, ChemOffice, VNMRJ, MestReNova/MestReC, Topspin, Spekwin32, Mendeley.
Interests and Hobbies	Travel, Sports (mountaineering, windsurfing, cardio), Music, Cooking, Photographing.
Professional expertise	**Organic and inorganic synthesis:** Strong background in synthetic chemistry including inert gas techniques and dry box handling. Diverse purification and characterization techniques for preparative scale experiments including column chromatography, preparative TLC and recrystallization of solid compounds. **Instrumental Analytics:** NMR-analysis, GC–MS, IR-spectroscopy, UV-VIS spectroscopy, Thermal conductivity analysis, Dynamic Light Scattering, DSC-TGA measurements, SEM-EDX measurements.
Social skills	**Good communication and presentation skills:** Gained through experience as a sports instructor and trainer and teaching assistant; Completion of seminars (Rhetoric & Presentation; Presentation techniques) and habitual research presentations at weekly group meetings and conferences. **Well organized and flexible:** Gained through self-reliant work in the laboratory and office and the completion of different tasks during work whilst running experiments simultaneously. **Self-dependent as well as the ability to work in a team:** Gained through the regular exposure to various personality types during work and free time. Quick decision making, patience, assess capabilities and the ability to take responsibility for the safety and training of team members are gained from years of mountaineering. **Drivers license.**

SCIENTIFIC RECORD

POSTER PRESENTATIONS AT CONFERENCES

1   Rausch Martin, Haas Michael, Hasken Bernd, Torvisco Ana and Stüger Harald: "Photoinduced Brook-type Rearrangement of Acylcyclosilanes", **15. Österreichische Chemietage**, September 24th, 2013, Graz, Austria.

ORAL PRESENTATIONS

1   Rausch Martin: „Photoinduced Rearrangement of cyclic Acylsilanes",
**6. Deutsch-Österreichischer Mitarbeiterworkshop
Hauptgruppenelement Chemie,** April 5th, 2013, Bonn, Deutschland.

2   Rausch Martin: „Synthesis of exo- and endocyclic Si-C-double bonds via Brook-type Rearrangement", **8. Workshop Anorganischer Chemie Österreich,** April 15th, 2014, Salzburg, Österreich.

PUBLICATIONS IN PEER REVIEWED JOURNALS

1   Stüger, Harald; Hasken, Bernd; Haas, Michael; Rausch, Martin; Fischer, Roland; Torvisco, Ana; "Photoinduced Brook-Type Rearrangement of Acylcyclopolysilanes", Organometallics, **2014**, 33 (1), 231–239.

2   Michael Haas, Roland Fischer, Michaela Flock, Stefan Mueller, Martin Rausch, Robert Saf, Ana Torvisco, Harald Stüger; "Stable Silenolates and Brook-Type Silenes with Exocyclic Structures", Organometallics, **2014**, 33 (21), 5956–5959.